

1 **The complex three-dimensional organization of epithelial**  
2 **tissues**

3  
4 Pedro Gómez-Gálvez<sup>1,2,†</sup>, Pablo Vicente-Munuera<sup>1,2,†</sup>, Samira Anbari<sup>3</sup>, Javier  
5 Buceta<sup>4,\*</sup>, Luis M. Escudero<sup>1,2,\*</sup>

6  
7 †: These authors contributed equally to this work.

8 \*: Corresponding authors

9  
10  
11 1: Instituto de Biomedicina de Sevilla (IBiS), Hospital Universitario Virgen del  
12 Rocío/CSIC/Universidad de Sevilla and Departamento de Biología Celular,  
13 Universidad de Sevilla. 41013 Seville, Spain.

14 2: Biomedical Network Research Centre on Neurodegenerative Diseases  
15 (CIBERNED), Madrid, Spain.

16 3: Chemical and Biomolecular Engineering Department, Lehigh University.  
17 Bethlehem, PA 18018, USA.

18 4: Institute for Integrative Systems Biology (I2SysBio), CSIC-UV, Paterna  
19 (Valencia), Spain.

20

1 **SUMMARY**

2 Understanding the cellular organization of tissues is key to developmental  
3 biology. In order to deal with this complex problem, researchers have taken  
4 advantage of reductionist approaches that have revealed fundamental  
5 morphogenetic mechanisms and quantitative laws. For epithelia, their two-  
6 dimensional representation as polygonal tessellations has been proved  
7 successful for understanding tissue organization. Yet, epithelial tissues bend  
8 and fold to shape organs in three dimensions. In this context, epithelial cells are  
9 too often simplified as prismatic blocks with a limited plasticity. However, there  
10 is increasing evidence that a realistic approach, even from a reductionist  
11 perspective, must include apico-basal intercalations (i.e. scutoidal cell shapes)  
12 for explaining epithelial organization convincingly. Here, we present an historical  
13 perspective about the tissue organization problem. Specifically, we analyse past  
14 and recent breakthroughs, and discuss how and why simplified, but realistic, *in*  
15 *silico* models require scutoidal features to address key morphogenetic events.

16

17

18 **KEYWORDS:** three-dimensional cell packing, cell shape, scutoid, apico-basal  
19 cell intercalation, mathematical modeling, biophysical modeling.

20

21

22

23

24

25

26

27

28

29

30

31

32

33

34

## 1 **Introduction**

2

3 The invention of the microscope led to the discovery of the fundamental unit of  
4 life: the cell. Yet, the collective organization of cells in tissues is far from obvious  
5 under the microscope and requires the combination of reliable staining methods  
6 and detailed analyses. For example, the neuron doctrine that set the  
7 foundations of modern neuroscience was only possible due to the combination  
8 of the staining method developed by Golgi (Golgi, 1885) and the histological  
9 analyses (and artistic talent) of Ramón y Cajal (de Castro et al., 2007; Ramón y  
10 Cajal, 1888; Ramón y Cajal, 1899) that in fact shared, for the first time, the  
11 Nobel prize in Medicine and Physiology.

12 Packed tissues, such as epithelia, pose additional problems at the time of  
13 elucidating the cellular organization since it is difficult to obtain detailed three-  
14 dimensional (3D) cellular shapes. This has led to the adoption of diverse  
15 reductionist approaches to understanding the epithelial tissue organization. The  
16 polygonal-like shape of epithelial cells on the apical surface of tissues is the  
17 source of the most important and prevalent simplification: epithelial cells have a  
18 prismatic-like shape (**Fig. 1A**). Thus, textbooks have traditionally depicted  
19 schematically the cells of epithelial monolayers as prisms with polygonal bases  
20 representing their apical and basal surfaces (Boyle, 2008; Gilbert, 2013). In the  
21 case of complex tissue rearrangements (e.g. folding and bending of epithelia)  
22 cells have been also represented by prismatic shapes. Still, under those  
23 circumstances, the cells necessarily reduce one of the polygonal surfaces  
24 (apical or basal) to accommodate to the curvature of the tissue (**Fig. 1B**). The  
25 term 'bottle shape' was coined to describe the cell shape that corresponds,  
26 geometrically speaking, to a truncated pyramid also known as 'frustum'  
27 (Schneider and Eberly, 2003). Epithelial cells with a bottle shape do appear  
28 during the invagination processes that occur during embryo development, such  
29 as gastrulation or the formation of the neural tube in vertebrates (Davidson,  
30 2012; Lecuit and Lenne, 2007; Pearl et al., 2017). An important implication of  
31 the 'prismatic simplification' is that apical and basal surface bases necessarily  
32 have the same number of sides (but may differ in size in the case of bottle-  
33 shaped cells). Consequently, such representation assumes tacitly that it is

1 enough to know the organization of the apical layer to understand the global 3D  
2 architecture and the cellular connectivity. Thus, until very recently, most studies  
3 have inferred the 3D organizational and biophysical information of epithelia by  
4 examining and modelling the apical cell surface alone. However, the natural  
5 shape of the epithelial cells is far more complex. In particular, several works  
6 have revealed the existence, predominantly in curved tissues, of apico-basal  
7 intercalations that challenge the idea of prismatic epithelial cells (**Fig. 1C**). This  
8 feature appears to be essential to understand dynamical events in different  
9 morphogenetic processes and to shed light into the biophysical forces that drive  
10 homeostatic epithelial packing. We notice that although cell-cell contacts are far  
11 from being straight in a number of well-studied epithelia, as shown, for example,  
12 by the curvature of the lateral membranes of columnar cells, here, we discuss  
13 efforts to develop reductionist representations of tissues based on "simple", yet  
14 faithful, representations of cell shapes away, in some cases, from the prismatic-  
15 like paradigm. Thus, we review the study of epithelial organization from a  
16 historical perspective and argue that such methodological approaches are  
17 particularly required for the implementation of computational models. These  
18 models, still limited, are extremely helpful to unveil the underlying biophysical  
19 cues driving morphogenesis.

20

## 21 **A historical perspective on the 3D epithelial organization**

22 The structure and cellular organization of developing tissues have been  
23 studied since the development of the first microscopes. Interestingly, the term  
24 'cell' was in fact coined in 1655 by Hooke when describing the organization of a  
25 tissue rather than an individual entity. Thus, when describing his observations  
26 under the microscope of thin slices of cork in 'Observation XVIII' of his  
27 celebrated book *Micrographia*, he wrote that this tissue resembled 'much like a  
28 Honey-comb, but the pores of it were not regular; [...] these pores, or *cells* [...]'  
29 (Hooke, 1665). Still, it was not until the 19<sup>th</sup> century that the cell theory was  
30 widely accepted and experimental embryology began to flourish, during which  
31 the question of how cells collectively organize became paramount. Soon  
32 enough, embryologists acknowledged that the cells were necessarily under the  
33 influence of the physical laws that govern nature. Robert, in 1903, thoroughly

1 analysed the early changes of the development of embryos of the genus  
2 *Trochus* (marine univalve mollusc) from this perspective (Robert, 1903).  
3 Typically, a four-cell embryo is composed of two lateral cells contacting two  
4 central cells, such that the central cells make contact between them and also  
5 with the lateral ones. However, Robert found cellular configurations where all  
6 four cells were sharing surface contacts (**Fig. 2**). To understand the processes  
7 leading to these configurations, Robert pioneered the usage of biophysically-  
8 inspired models based on soap bubble experiments. Thus, he studied the 3D  
9 structures derived from four-bubble motifs by perturbing the force equilibrium  
10 (e.g. in motifs where the bubbles had the same volume) by removing air from  
11 the two bubbles at the end of the polar furrow (lateral cells). With these  
12 experiments, he was able to reproduce the different configurations observed in  
13 real embryos (**Fig. 2**). He then concluded that surface tension was the most  
14 important physical phenomenon underlying the organization of both cells and  
15 foam bubbles. Years later, the mathematical biologist Sir D'Arcy Thompson, in  
16 his seminal book *On Growth and Form* (Thompson, 1917), remarked the  
17 presence of the configurations analysed by Robert and added other  
18 configurations found in embryos of different animals, such as the starfish (genus  
19 *Asterina*) (Ludwig, 1882) or the freshwater anostracan (genus *Branchipus*)  
20 (Spangenberg, 1875), and pollen-grains of orchids (genus *Neottia*) (Goebel et  
21 al., 1887) (**Fig. 2**).

22 Parallel to these efforts, in 1887 Lord Kelvin proposed a solution to the classic  
23 problem of dividing the space with cells with minimum surface area. He  
24 introduced the idea of 14-sided shapes, or 'tetrakaidecahedral' cells, and  
25 demonstrated their appearance in soap-films (Thomson, 1887) (**Fig. 2**). Later,  
26 Frederic T. Lewis made a careful study that considered the possibility that such  
27 a shape was present in the cells of ordinary vegetable parenchyma (specifically,  
28 in *Sambucus canadensis*) (Lewis, 1923). Lewis examined quantitatively the  
29 cellular 3D contacts and observed cells with a diverse number of sides and  
30 conformations. Notably, he found predominantly 14-sided cells as Kelvin  
31 predicted, thus validating, indirectly, that surface tension was the main driver of  
32 cellular organization. Lewis also observed later the same prevalence of the  
33 tetrakaidecahedral shape in human fat cells (Lewis, 1925) (**Fig. 2**) and in the

1 precartilate tadpole of the common toad (*Bufo lentiginous*) (Lewis, 1933).  
2 Moreover, Marvin confirmed the presence of the tetrakaidecahedron in metal  
3 (using compressed lead shots) (Marvin, 1939a), and in the pith of the weed  
4 *Eupatorium purpureom* (Marvin, 1939b). Altogether, these studies suggested  
5 that similar physical principles led to the same geometric configurations in living  
6 tissues, inert froths, and even metals.

7 Subsequent advances in microscopy allowed scientists to dig deeper into the  
8 knowledge of 3D cell shapes and tissue organization. Importantly, it became  
9 possible not only to study the cell packing of complex organs, but also its  
10 relationship to the underlying developmental processes. In 1976, Menton  
11 described in detail the cell packing of the parenchymal cells of *Cork cambium*  
12 (from commercial cork bottle stoppers), the pith of shrub stems (*Sambucus*  
13 *canadensis*) and the stratified epithelium of one of the epidermal layers of the  
14 mouse inner ear (Allen and Potten, 1976; Menton, 1976). He found that the cell  
15 arrangements of these very diverse organisms were ‘universally’ formed by  
16 columns of flattened 14-sided cells once again (**Fig. 2**) (Allen and Potten, 1976;  
17 Menton, 1976). In fact, a recent work (Yokouchi et al., 2016) revisited the  
18 problem of the organization of epithelial cells in the mouse ear skin by using *in*  
19 *vivo* live imaging and computational models (**Fig. 2**). The authors corroborated  
20 previous experiments and highlighted that the flattened Kelvin’s  
21 tetrakaidecahedron is indeed the optimal shape to fill the space of this stratified  
22 epithelium. In biological terms, the authors suggested that these cell structures  
23 promote an accurate barrier to maintain homeostasis and, in addition, increase  
24 the physical strength of this tissue.

25 The relationship between cell morphology and its primary role in  
26 morphogenetic events was also an object of study in monolayer epithelia. In this  
27 context, it is worth mentioning the investigation carried out by Condic and  
28 colleagues (Condic et al., 1991) (**Fig. 2**). In their study, the elongation of the  
29 *Drosophila* leg imaginal disc was analysed from the perspective of cellular  
30 organization. Importantly, by comparing the cellular organization of apical and  
31 basal surfaces, it was shown that the cells did not preserve the same number of  
32 neighbours. These findings thus revealed, indirectly, the existence of apico-  
33 basal intercalations (**Glossary**) that challenged, for the first time, the ‘prismatic

1 simplification' in an epithelia monolayer (**Fig. 1B,C; Fig. 2**). On the  
2 computational side, it was not until 2008 when Honda and colleagues  
3 developed the first 3D model that suggested transient apico-basal intercalations  
4 as a way to enable tissue elongation (Honda et al., 2008) (**Fig. 2**). Additional  
5 experimental studies have subsequently revealed – either directly or indirectly –  
6 these non-prismatic epithelial shapes in different tissue monolayers. Thus, cell-  
7 neighbouring changes between apical and basal surfaces (non-compatible with  
8 prism-like cells) were also reported on the Wolffian duct epithelium in mouse  
9 (Xu et al., 2016). Notably, from a dynamics viewpoint, Sun and colleagues  
10 demonstrated that during the *Drosophila* germ-band extension the active tissue  
11 elongation was driven by basolateral protrusions and transient apico-basal  
12 intercalations among cells (Sun et al., 2017) (**Fig. 2**). More recently, these  
13 dynamical intercalations have been shown to be relevant in different contexts,  
14 such as the development of the salivary glands placode in *Drosophila*  
15 (Sanchez-Corrales et al., 2018) and during the *Drosophila* embryo  
16 cellularization (Rupprecht et al., 2017) (**Fig. 2**). Finally, the mathematical  
17 formalization of a novel geometrical shape in connection to the apico-basal  
18 intercalations, the scutoid, uncovered important biophysical consequences for  
19 the 3D tissue organization (Gómez-Gálvez et al., 2018) (**Fig. 1C**). In particular,  
20 it was suggested, for the first time, how the thickness and curvature of tissues  
21 modulate the appearance of apico-basal intercalations. Additionally, it was  
22 proposed that the underlying motive for this new shape, was to minimize  
23 surface energy expenditure when tissues are subjected to anisotropic bending.  
24 This hypothesis was further confirmed by a study in froth monolayers that  
25 revived the idea of the surface tension as the main driver of cellular organization  
26 in the context of epithelial monolayers (Mughal et al., 2018) (**Fig. 2**).

27

## 28 **The mathematics and biophysics of epithelial organization**

### 29 Mathematical tools/laws to quantify epithelial organization

30 One important advantage of the 'prismatic' approximation is that it makes it  
31 possible to implement common elements of mathematical topology to  
32 investigate tissue packing. In particular, the analysis of the topology of the

1 apical surface of epithelia has provided useful information about metazoan  
2 development. Reinhart used Euler's principle for convex polyhedrons, Vertices-  
3 Edges+Faces=2 (Glossary) (Euler, 1767), to formally deduce that the average  
4 number of sides of the cells in a plane tessellation of convex polygons should  
5 be six (Reinhardt, 1918) (Fig. 3A,B). Later, this conclusion was experimentally  
6 confirmed in epithelia by Wetzel (Wetzel, 1926).

7 Lewis further analysed tissues from a geometrical and topological viewpoint,  
8 and established the existence of a linear relationship between the average cell  
9 areas and the number of neighbours (Lewis, 1928) (Fig. 3C). Rivier and  
10 Lissowski subsequently demonstrated mathematically that the so-called 'Lewis'  
11 law' (Glossary) originates in a maximum entropy principle given the constraints  
12 of the cellular topology (Rivier and Lissowski, 1982). The Lewis' law was  
13 successfully confirmed afterwards in a number of biological tissues and two-  
14 dimensional (2D) Voronoi tessellations (Glossary) (Farhadifar et al., 2007;  
15 Gibson et al., 2006; Sánchez-Gutiérrez et al., 2016). In relation with the  
16 similarities between Voronoi diagrams and epithelial tissues, a breakthrough  
17 was established in 1978, when Honda and colleagues showed that the Voronoi  
18 compartmentalization of a 2D space fitted well the pattern of cellular contacts  
19 found in epithelial surfaces (Honda, 1978).

20 Another example of a mathematical principle observed in convex  
21 tessellations of the plane is the Aboav-Weaire's law (Glossary) that states an  
22 inverse relationship between the mean number of sides of the neighbours of a  
23 cell and its number of neighbours (Aboav, 1970; Chiu, 1995) (Fig. 3D). This law  
24 was first observed in the grains of growing polycrystals but was also satisfied in  
25 2D Voronoi tessellations (Glossary) (Zhu et al., 2001) and in the apical plane of  
26 growing epithelia (Bi et al., 2014; Sánchez-Gutiérrez et al., 2016).

27 The aforementioned principles and properties refer to statistical moments  
28 (e.g. averages), but the details of the underlying polygonal distribution have  
29 been also the focus of research. Thus, Lewis quantified for the first time the  
30 polygonal distribution of cells in the *Cucumis* epidermis (Lewis, 1928). More  
31 recently, a seminal work by Gibson and colleagues demonstrated that the origin  
32 of a conserved polygonal distribution of cells among Metazoa is a consequence  
33 of cell proliferation (Gibson et al., 2006) (Fig. 3E). Subsequent studies



1 introduced elements of Graph Theory ([Glossary](#)) to analyse the polygonal  
2 distribution of cell contacts and to quantify in some cases the epithelial topology  
3 under physiological and pathological conditions (Escudero et al., 2011; Kursawe  
4 et al., 2016; Sanchez-Gutierrez et al., 2013; Vicente-Munuera et al., 2020;  
5 Yamashita and Michiue, 2014). Other complementary methods combined the  
6 polygon distribution analysis with the application of *in silico* models, such as  
7 vertex models ([Glossary](#)) or [Voronoi tessellations](#), trying to reproduce and  
8 explain the biological behaviour by mathematical/computational means (Aland  
9 et al., 2015; Bi et al., 2016; Curran et al., 2017; Farhadifar et al., 2007). These  
10 analyses suggested that the conserved metazoan polygon distribution was not  
11 exclusively dependent on cell division mechanisms, but a consequence of the  
12 physical restrictions found in natural tessellations and of the homogeneous size  
13 of the epithelial cells (Sánchez-Gutiérrez et al., 2016).

14 The mathematical principles and properties described above were assumed  
15 to be valid in a 3D context in epithelial monolayers given the ‘prismatic  
16 simplification’. However, the unveiling of cellular scutoidal shapes challenges  
17 some of these organizational principles. We envision further generalizations of  
18 the mathematical organizational principles to a 3D context in the future years  
19 (see Discussion) (**Fig. 3A–F**).

20

### 21 Forces and stresses inference

22 A mechanistic approach towards developmental biology ultimately seeks to  
23 elucidate the forces that drive cellular shapes and their collective properties.  
24 Such knowledge is required for developing realistic, predictive modeling  
25 frameworks and, ultimately, to understand the determinants of the  
26 organizational and mathematical features displayed by tissues. During the last  
27 few decades, different approaches have been developed to characterize forces  
28 and stresses at the cellular and collective levels, both in 2D and in 3D (Gómez-  
29 González et al., 2020; Roca-Cusachs et al., 2017; Sugimura et al., 2016; Xu et  
30 al., 2018). In this context, geometric force inference (GFI) methods are of  
31 special interest to understand epithelial organization. This methodology is  
32 based on either imposing a force equilibrium on the vertices that define either  
33 the polygonal (2D) or prismatic-like (3D) shapes of cells, or on applying the

1 Young-Laplace formula (Glossary) to balance the normal stresses (Fig. 4A).  
2 While GFI has limitations (e.g. only relative values of tensions and pressure  
3 differences can be estimated), it also has many advantages (e.g. it is non-  
4 invasive) and has been instrumental to understand a number of morphogenetic  
5 events (Gómez-González et al., 2020; Noll et al., 2020; Sugimura et al., 2016;  
6 Vasan et al., 2019; Veldhuis et al., 2017). Notably, GFI has traditionally focused  
7 on the 2D cellular organization of tissues and, to our knowledge, only two recent  
8 works have proposed a 3D extension (Veldhuis et al., 2017; Xu et al., 2018).  
9 Veldhuis and colleagues introduced CellFIT-3D, a tool based on the inference  
10 of 3D properties using 2D slides (e.g. confocal images). This approach avoids  
11 the methodological bottleneck of cellular reconstruction and has been also  
12 proposed to derive statistical properties of the 3D cell geometry in tissues  
13 (Sharp et al., 2019). More recently, normal stresses and tensions have also  
14 inferred in 3D to better understand the cellular organization in the early *C.*  
15 *elegans* embryo (Xu et al., 2018). However, as of today, no GFI approach has  
16 been used to infer forces in 3D epithelial monolayers where apico-basal  
17 intercalations develop. One of reasons lies in the lack of a precise  
18 characterization of the existing lateral cell-cell interactions. Consequently,  
19 besides the proposal that line/surface tension plays a key role in determining  
20 novel cellular geometries in curved 3D environments (Gómez-Gálvez et al.,  
21 2018; Mughal et al., 2018), there is still a gap of knowledge about how the  
22 balance of different acting forces (e.g. contractility versus adhesion) lead to a  
23 cellular organization in 3D. In that regard, further advances in the  
24 implementation of the microbulge technique (controlled formation and  
25 manipulation of tissue domes and, possibly, of other 3D tissue micropatterns)  
26 might shed light into this problem (Latorre et al., 2018). This methodology  
27 allows to control the remodelling of cellular and tissue shapes in 3D and to  
28 correlate those changes with the acting forces and a compatible cellular  
29 mechanics. In particular, the authors of this study, by using a 3D biophysical  
30 tissue model, were able to reveal the so-called ‘active super-elasticity  
31 phenomenon’ in bent epithelial monolayers: cells have the capability to deform,  
32 reversibly, at a constant tension. This example highlights the importance for  
33 developing convincing biophysical tissue models (see below), and the need to

1 develop and implement realistic force inference methods to 3D epithelia, in  
2 order to unveil the processes that control 3D tissue organization.

3

#### 4 Epithelia simulation models: from 2D to 3D

5 Modern developmental biology is built upon the combined effort of novel  
6 biological techniques and computational approaches in order to describe the  
7 biological and biophysical behaviour of tissues. Following this trend, the field is  
8 experiencing a slow, yet steady, evolution towards the study of tissues from a  
9 more realistic perspective. Specifically, 2D simulations have contributed  
10 enormously to the progress of the field, but the next step is the implementation  
11 of 3D simulation schemes that make possible to understand how animals  
12 develop in a four dimensional context (three spatial dimensions + time). Here  
13 we describe major advances in the context of 2D simulation models and  
14 elaborate about the challenges for implementing 3D computational approaches.

15 There is a great number of cell-based computational solutions towards the  
16 simulation of tissues (Fletcher and Osborne, 2020; Metzcar et al., 2019). They  
17 are particularly useful for describing epithelia: they are computationally efficient  
18 and allow to make direct comparisons with GFI methods by describing the  
19 acting forces on cell connectivity loci. Honda and Eguchi laid the foundations of  
20 the ‘vertex model’ by showing that cell boundary contraction processes in the  
21 surface of epithelia could be described by a model of packed convex polygons  
22 with an area-conservation property (Honda and Eguchi, 1980). Later, Nagai and  
23 Honda formalized the model by proposing a simulation technique that linked the  
24 polygonal geometry of cells in epithelial surfaces with the forces acting at cell  
25 vertices (Nagai and Honda, 2001). This seminal study showed that a  
26 deterministic approach that included line-tension and elastic force terms,  
27 together with topological changes (T1 transitions), was enough to describe the  
28 organization in epithelia in equilibrium. Further developments of the vertex  
29 model have included, on the one hand, additional mechanical effects, such as  
30 contractility force terms due to the acto-myosin ring (Farhadifar et al., 2007) or  
31 to anisotropies in acto-myosin activity (Canela-Xandri et al., 2011) (**Fig. 4B**). On  
32 the other hand, it has been shown that non-equilibrium contributions due to

1 migration, cellular proliferation, and oriented cell divisions can explain  
2 transitions from soft to solid phases in tissues (Farhadifar et al., 2007), jamming  
3 transitions (Bi et al., 2016), remodelling at the tissue level (Anbari and Buceta,  
4 2020; Mao et al., 2011), the appearance of pathological and mutant conditions  
5 deviating from tissue homeostasis (Ramanathan et al., 2019; Sánchez-  
6 Gutiérrez et al., 2016), or wound-healing processes (Staddon et al., 2018;  
7 Tetley et al., 2019). Recent developments of the vertex model have also  
8 included viscoelastic and mechanosensitive effects (Canela-Xandri et al., 2020;  
9 Staddon et al., 2019). All these studies have shown that the aforementioned  
10 mathematical laws accomplished by real epithelia are satisfied by vertex model  
11 simulations thus providing additional support to this computational method  
12 **(Fig. 3,4)**.

13 During the last few years, a number of modifications of the vertex model have  
14 been proposed, aimed at adapting this simulation methodology to more  
15 complex geometries. For example, simulations of 2D cross-sections along the  
16 apico-basal axis of curved epithelial monolayers have been used to study  
17 *Drosophila*'s ventral furrow formation (Polyakov et al., 2014) or the buckling and  
18 folding of cell cultures (Merzouki et al., 2018). Also, vertex models have been  
19 modified to simulate either the apical or the basal surfaces of curved tissues.  
20 Some examples include the dorsal appendage formation in the egg chamber  
21 (Osterfield et al., 2013), epithelial folding (Monier et al., 2015), and the  
22 tubulogenesis process (Hirashima and Adachi, 2019).

23 The generalization of the vertex model to 3D poses some challenges. To  
24 start, an accurate description of the tissue behaviour must account for the  
25 mechanical polarization of cells along the apico-basal axis. This implies the  
26 need to prescribe distinct mechanical interactions among cells in apical and  
27 basal surfaces and through the lateral contacts. In addition, the possible effects  
28 of the extracellular matrix become more relevant. Finally, the computational  
29 implementation of some cellular processes that shape tissues, such as growth,  
30 division, apico-basal intercalations, and/or extrusion/apoptosis, become more  
31 complex.

32 In this context, some attempts have been made to generalize the vertex  
33 model to a 3D environment. The first 3D vertex model was proposed by Honda

1 and colleagues to simulate cell aggregates (Honda et al., 2004). Further  
2 implementations have been used in the context of epithelial monolayers to  
3 simulate proliferation, deformation and invagination during morphogenesis  
4 (Bielmeier et al., 2016; Du et al., 2014; Inoue et al., 2020; Misra et al., 2016;  
5 Okuda et al., 2015; Okuda et al., 2018a; Sui et al., 2018), as well as branching  
6 growth (Okuda et al., 2018b), microbulge dome dynamics (Latorre et al., 2018),  
7 tubulogenesis (Inaki et al., 2018; Inoue et al., 2016), tumour progression  
8 (Messal et al., 2019), and 3D buckling instabilities in epithelial monolayers  
9 (Hannezo et al., 2014). For additional information about the foundations of the  
10 vertex model, both in 2D and 3D and other examples about its applicability to  
11 morphogenesis we refer the reader to the following studies (Alt et al., 2017;  
12 Fletcher et al., 2014). However, regardless of the progress achieved thanks to  
13 the vertex model to understand the link between energetic traits (i.e. forces) and  
14 epithelial organization, all the aforementioned studies disregard apico-basal  
15 intercalations. On top of the early work of Honda and colleagues (Honda et al.,  
16 2008), some recent exceptions include the work by Okuda and colleagues that  
17 suggests that scutoids may develop during cell rearrangements due to  
18 fluctuations and an asymmetry between the line tension of apical and basal  
19 surfaces (Okuda et al., 2019). We argue that these sort of modeling approaches  
20 along with novel, hybrid, simulations schemes are a must to describe accurately  
21 the 3D epithelial organization and shed light into the forces involved (especially  
22 in the context of curved tissues) (**Fig. 4B**). By hybrid simulation schemes we  
23 mean computational methods that combine, on the one hand, the simplicity of  
24 the vertex model such that can be easily parametrized by force inference  
25 methods (i.e. GFI). On the other hand, these novel methods must include  
26 enough complexity elements to generate the observed self-organization in  
27 tissues containing complex cellular geometries. Some recent promising results  
28 have been shown by Ioannou and colleagues, that have proposed a  
29 methodology that accounts for the reported asymmetries between apical and  
30 basal surfaces, and applied it to study wound healing (Ioannou et al., 2020).

31

## 32 **Discussion and conclusions**

33 For over a century, the morphology of the cells has intrigued researchers from  
34 different fields. In *On Growth and Form*, D'Arcy W. Thompson made a unifying,

1 quantitative effort and put together the accumulated knowledge from different  
2 fields to understand the basis of shape establishment. In this way, he linked the  
3 complex process of morphogenesis to the emergence of mathematical patterns  
4 and the physical nature of cells. Notably, in many of these pioneering works that  
5 he compiled, there was an exquisite description of the three-dimensional shape  
6 of the cells. These depictions included artistic drawings and quantitative  
7 approaches that helped to infer the physics underlying the formation of shapes  
8 (**Fig. 2**). Now, researchers have far more microscopy resources than in D'Arcy  
9 W. Thompson's day to explore and analyse in depth the form of cells, their  
10 dynamic changes, and how they integrate within tissues. Interestingly, these  
11 advances in microscopy have led to a re-examination of some of the  
12 phenomena presented by D'Arcy W. Thompson. In parallel to this experimental  
13 progress, different computational tools have been designed to model  
14 morphogenetic processes. These tools are based on reductionist approaches  
15 that capture the essential biophysical cues and mathematical principles that  
16 drive tissue shape and cellular organization. Together, these tools aim to find  
17 'universality' in developmental processes, as D'Arcy W. Thompson aspired to as  
18 well.

19 As reviewed here in the context of epithelial morphogenesis, most studies that  
20 have analysed tissue organization and its biophysics have limited the study to a  
21 single epithelial surface. While informative and extremely useful, these  
22 investigations also neglect the realistic 3D cellular shapes in monolayer tissues.  
23 Moreover, only a few examples have analysed the organization of stratified  
24 epithelia (**Fig. 2**). These two aspects are promising research challenges in the  
25 field. In this Review, we have particularly focused on single layer epithelia  
26 development, that we identify as the first – and easiest – step to design realistic  
27 *in silico* tools coupled to force inference methods. To that end, on the one hand,  
28 further progress is needed to elucidate the forces that determine the epithelial  
29 organization in 3D. On the other hand, the parametrization and calibration of  
30 *in silico* models must be consistent with those force estimations. Fortunately,  
31 recent results seem to suggest that realistic 3D tissue organizational traits, such  
32 as the scutoidal shapes, can be reproduced in force-driven models without  
33 implementing excessive complexity (Okuda et al., 2019, Ioannou et al., 2020).

1 This will facilitate the exploration of dynamical phenomena in the near future,  
2 because apico-basal intercalations also appear involved in active cell  
3 movements, such as the *Drosophila* germ band extension, egg chamber  
4 rotation, or the early morphogenesis of salivary glands (Gómez-Gálvez et al.,  
5 2018; Sanchez-Corrales et al., 2018; Sun et al., 2017). Another equally  
6 important avenue of research is the influence of the global tissue shape on the  
7 3D cellular packing of epithelia. Recent results by Saunders' lab described a  
8 relationship between curvature and the emergence of apico-basal intercalations  
9 on the curved tips of the *Drosophila* embryo (Rupprecht et al., 2017). This  
10 phenomenon was later generalized through computational models and  
11 experiments to show that the appearance of scutoids is directly dependent on  
12 the anisotropy of the tissue curvature, and scutoids are more frequently  
13 observed in tubular epithelia (Gómez-Gálvez et al., 2018).

14 Further progress in understanding 3D tissue organizational relies on the  
15 advances in microscopy to obtain high-resolution imaging of epithelia and  
16 provide precise information of 3D and 4D cell conformations. In combination  
17 with improvements in machine learning techniques aimed at performing fixed-  
18 and live-tissue segmentation, these methodologies will soon allow realistic  
19 elucidation of the cellular changes that drive morphogenesis (Arganda-Carreras  
20 et al., 2017; Chamier et al., 2020; Falk et al., 2019; Haberl et al., 2018; Lee et  
21 al., 2020; Wolny et al., 2020). Moreover, the precise quantification of the 3D  
22 tissue structure in epithelia will enable the study of quantitative principles and  
23 mathematical laws that, so far, have only been tested in 2D planar epithelia. We  
24 stress that the advantage of these quantitative principles lies in their ability to  
25 identify biological functionalities in homeostasis (Escudero et al., 2011;  
26 Farhadifar et al., 2007; Gibson et al., 2006) and in pathological conditions  
27 (Sánchez-Gutiérrez et al., 2016; Tsuboi et al., 2018). Interestingly, there are  
28 already promising 3D approaches modelling cancer disease in tubular  
29 geometries (Messal et al., 2019). Unfortunately, the 'prismatic simplification' has  
30 led to the (wrong) assumption that some of these principles are automatically  
31 satisfied in 3D. However, there are some clear examples that it is not the case.  
32 Specifically, the average number of cellular neighbours in 3D (i.e. the average  
33 cellular connectivity) cannot possibly be six if apico-basal intercalations occur

1 (Euler, 1767; Reinhardt, 1918). In this regard, recent studies have highlighted  
2 the importance of cellular connectivity in different developmental contexts, such  
3 as supervising neuroepithelial morphogenesis (Sharma et al., 2019), or  
4 controlling cell fate decisions (Guignard et al., 2020). Interestingly, one study  
5 has recently uncovered the principle that describes how scutoids modify the 3D  
6 cellular connectivity: the Flintstones' law ([Glossary](#)) (Gomez-Galvez et al.,  
7 2020) (**Fig. 3F**). We anticipate that there will be additional discoveries of  
8 quantitative principles in the context of 3D cellular organization in the years to  
9 come, which will help to justify D'Arcy W. Thompson's claim: '*The harmony of  
10 the world is made manifest in Form and Number, and the heart and soul and all  
11 the poetry of Natural Philosophy are embodied in the concept of mathematical  
12 beauty*'.

13 Some final words refer to promising applications to the field of biomedicine.  
14 The possibility of generating human 3D cultures that resemble specific organs  
15 (organoids) has opened up enormous possibilities (Rossi et al., 2018; Tuveson  
16 and Clevers, 2019). However, recent advances in organoid technology,  
17 although highly promising, are hindered by its current lack of reproducibility  
18 (Huch et al., 2017). We believe that the combination of an accurate  
19 understanding about how the cells self-organize and pack in 3D, and the  
20 advances on the knowledge on how substrate curvature guide spatiotemporal  
21 cell and tissue organization (Callens et al., 2020), will help to control the growth  
22 of organoid cultures. Altogether, the realistic analysis of epithelial packing can  
23 also advance the biomedical field, especially in tissue and organ engineering  
24 (Hendow et al., 2016; Yin et al., 2016).



1 REFERENCES

- 2
- 3 **Aboav, D. A.** (1970). The arrangement of grains in a polycrystal. *Metallography*
- 4 **3**, 383–390.
- 5 **Aland, S., Hatzikirou, H., Lowengrub, J. and Voigt, A.** (2015). A Mechanistic
- 6 Collective Cell Model for Epithelial Colony Growth and Contact Inhibition.
- 7 *Biophys. J.* **109**, 1347–1357.
- 8 **Allen, T. D. and Potten, C. S.** (1976). Significance of cell shape in tissue
- 9 architecture. *Nature* **264**, 545–547.
- 10 **Alt, S., Ganguly, P. and Salbreux, G.** (2017). Vertex models: from cell
- 11 mechanics to tissue morphogenesis. *Philos. Trans. R. Soc. B Biol. Sci.*
- 12 **372**, 20150520.
- 13 **Anbari, S. and Buceta, J.** (2020). Self-sustained planar intercalations due to
- 14 mechanosignaling feedbacks lead to robust axis extension during
- 15 morphogenesis. *Sci. Rep.* **10**, 10973.
- 16 **Arganda-Carreras, I., Kaynig, V., Rueden, C., Eliceiri, K. W., Schindelin, J.,**
- 17 **Cardona, A. and Sebastian Seung, H.** (2017). Trainable Weka
- 18 Segmentation: a machine learning tool for microscopy pixel classification.
- 19 *Bioinformatics* **33**, 2424–2426.
- 20 **Bi, D., Lopez, J. H., Schwarz, J. M. and Lisa Manning, M.** (2014). Energy
- 21 barriers and cell migration in densely packed tissues. *Soft Matter* **10**, 1885–
- 22 1890.
- 23 **Bi, D., Yang, X., Marchetti, M. C. and Manning, M. L.** (2016). Motility-Driven
- 24 Glass and Jamming Transitions in Biological Tissues. *Phys. Rev. X* **6**,
- 25 021011.
- 26 **Bielmeier, C., Alt, S., Weichselberger, V., La Fortezza, M., Harz, H.,**
- 27 **Jülicher, F., Salbreux, G. and Classen, A.-K.** (2016). Interface
- 28 Contractility between Differently Fated Cells Drives Cell Elimination and
- 29 Cyst Formation. *Curr. Biol.* **26**, 563–574.
- 30 **Boyle, J.** (2008). Molecular biology of the cell, 5th edition by B. Alberts, A.
- 31 Johnson, J. Lewis, M. Raff, K. Roberts, and P. Walter. *Biochem. Mol. Biol.*
- 32 *Educ.* **36**, 317–318.
- 33 **Callens, S. J. P., Uyttendaele, R. J. C., Fratila-Apachitei, L. E. and Zadpoor,**
- 34 **A. A.** (2020). Substrate curvature as a cue to guide spatiotemporal cell and
- 35 tissue organization. *Biomaterials* **232**, 119739.
- 36 **Canela-Xandri, O., Sagués, F., Casademunt, J. and Buceta, J.** (2011).
- 37 Dynamics and Mechanical Stability of the Developing Dorsalventral
- 38 Organizer of the Wing Imaginal Disc. *PLoS Comput. Biol.* **7**, e1002153.
- 39 **Canela-Xandri, O., Anbari, S. and Buceta, J.** (2020). TiFoSi: an efficient tool
- 40 for mechanobiology simulations of epithelia. *Bioinformatics* **36**, 4525–4526.
- 41 **Chamier, L. von, Jukkala, J., Spahn, C., Lerche, M., Hernández-pérez, S.,**
- 42 **Mattila, P., Karinou, E., Holden, S., Solak, A. C., Krull, A., et al.** (2020).
- 43 ZeroCostDL4Mic: an open platform to simplify access and use of Deep-
- 44 Learning in Microscopy. *bioRxiv* 2020.03.20.000133.
- 45 **Chiu, S. N.** (1995). Aboav-Weaire's and Lewis' laws—A review. *Mater. Charact.*
- 46 **34**, 149–165.
- 47 **Condic, M. L., Fristrom, D. and Fristrom, J. W.** (1991). Apical cell shape
- 48 changes during *Drosophila* imaginal leg disc elongation: a novel
- 49 morphogenetic mechanism. *Development* **111**, 23–33.
- 50 **Curran, S., Strandkvist, C., Bathmann, J., de Gennes, M., Kabla, A.,**

- 1       **Salbreux, G. and Baum, B.** (2017). Myosin II Controls Junction  
2       Fluctuations to Guide Epithelial Tissue Ordering. *Dev. Cell* **43**, 480-492.e6.
- 3       **Davidson, L. A.** (2012). Epithelial machines that shape the embryo. *Trends*  
4       *Cell Biol.* **22**, 82–87.
- 5       **de Castro, F., López-Mascaraque, L. and De Carlos, J. A.** (2007). Cajal:  
6       Lessons on brain development. *Brain Res. Rev.* **55**, 481–489.
- 7       **Du, X., Osterfield, M. and Shvartsman, S. Y.** (2014). Computational analysis  
8       of three-dimensional epithelial morphogenesis using vertex models. *Phys.*  
9       *Biol.* **11**, 066007.
- 10       **Escudero, L. M., da F. Costa, L., Kicheva, A., Briscoe, J., Freeman, M. and**  
11       **Babu, M. M. M.** (2011). Epithelial organisation revealed by a network of  
12       cellular contacts. *Nat. Commun.* **2**, 526.
- 13       **Euler, L.** (1767). *Solutio facilis problematum quorundam geometricorum*  
14       *difficillimorum*. Novi Commentarii academiae scientiarum Petropolitanae.
- 15       **Falk, T., Mai, D., Bensch, R., Çiçek, Ö., Abdulkadir, A., Marrakchi, Y.,**  
16       **Böhm, A., Deubner, J., Jäckel, Z., Seiwald, K., et al.** (2019). U-Net: deep  
17       learning for cell counting, detection, and morphometry. *Nat. Methods* **16**,  
18       67–70.
- 19       **Farhadifar, R., Röper, J.-C., Aigouy, B., Eaton, S. and Jülicher, F.** (2007).  
20       The Influence of Cell Mechanics, Cell-Cell Interactions, and Proliferation on  
21       Epithelial Packing. *Curr. Biol.* **17**, 2095–2104.
- 22       **Fletcher, A. and Osborne, J.** (2020). Seven Challenges in the Multiscale  
23       Modelling of Multicellular Tissues.
- 24       **Fletcher, A. G., Osterfield, M., Baker, R. E. and Shvartsman, S. Y.** (2014).  
25       Vertex models of epithelial morphogenesis. *Biophys. J.* **106**, 2291–2304.
- 26       **Gibson, M. C., Patel, A. B., Nagpal, R. and Perrimon, N.** (2006). The  
27       emergence of geometric order in proliferating metazoan epithelia. *Nature*  
28       **442**, 1038–1041.
- 29       **Gilbert, S. F.** (2013). Developmental Biology. *Dev. Biol.*
- 30       **Goebel, K., Garnsey, H., Balfour, I. and Sachs, J.** (1887). *Outlines of*  
31       *classification and special morphology of plants.*
- 32       **Golgi, C.** (1885). Sulla fina anatomia degli organi centrali del sistema nervoso.  
33       *S. Calderini.*
- 34       **Gomez-Galvez, P., Vicente-Munuera, P., Anbari, S., Tagua, A., Gordillo, C.,**  
35       **Palacios, A. M., Velasco, A., Capitan-Agudo, C., Grima, C., Annese, V.,**  
36       **et al.** (2020). A quantitative principle to understand 3D cellular connectivity  
37       in epithelial tubes. *bioRxiv* 2020.02.19.955567.
- 38       **Gómez-Gálvez, P., Vicente-Munuera, P., Tagua, A., Forja, C., Castro, A. M.**  
39       **A. M., Letrán, M., Valencia-Expósito, A., Grima, C., Bermúdez-**  
40       **Gallardo, M., Serrano-Pérez-Higueras, Ó., et al.** (2018). Scutoids are a  
41       geometrical solution to three-dimensional packing of epithelia. *Nat.*  
42       *Commun.* **9**, 2960.
- 43       **Gómez-González, M., Latorre, E., Arroyo, M. and Trepát, X.** (2020).  
44       Measuring mechanical stress in living tissues. *Nat. Rev. Phys.* **2**, 300–317.
- 45       **Guignard, L., Fiúza, U.-M., Leggio, B., Laussu, J., Faure, E., Michelin, G.,**  
46       **Biasuz, K., Hufnagel, L., Malandain, G., Godin, C., et al.** (2020). Contact  
47       area-dependent cell communication and the morphological invariance of  
48       ascidian embryogenesis. *Science (80- )*. **369**, eaar5663.
- 49       **Haberl, M. G., Churas, C., Tindall, L., Boassa, D., Phan, S., Bushong, E. A.,**  
50       **Madany, M., Akay, R., Deerinck, T. J., Peltier, S. T., et al.** (2018).

- 1 CDeep3M—Plug-and-Play cloud-based deep learning for image  
2 segmentation. *Nat. Methods* **15**, 677–680.
- 3 **Hannezo, E., Prost, J. and Joanny, J. F.** (2014). Theory of epithelial sheet  
4 morphology in three dimensions. *Proc. Natl. Acad. Sci. U. S. A.* **111**, 27–  
5 32.
- 6 **Hendow, E. K., Guhmann, P., Wright, B., Sofokleous, P., Parmar, N. and**  
7 **Day, R. M.** (2016). Biomaterials for hollow organ tissue engineering.  
8 *Fibrogenesis Tissue Repair* **9**, 3.
- 9 **Hirashima, T. and Adachi, T.** (2019). Polarized cellular mechano-response  
10 system for maintaining radial size in developing epithelial tubes.  
11 *Development* **146**, dev181206.
- 12 **Honda, H.** (1978). Description of cellular patterns by Dirichlet domains: the two-  
13 dimensional case. *J Theor Biol* **72**, 523–543.
- 14 **Honda, H. and Eguchi, G.** (1980). How much does the cell boundary contract  
15 in a monolayered cell sheet? *J. Theor. Biol.* **84**, 575–588.
- 16 **Honda, H., Tanemura, M. and Nagai, T.** (2004). A three-dimensional vertex  
17 dynamics cell model of space-filling polyhedra simulating cell behavior in a  
18 cell aggregate. *J. Theor. Biol.* **226**, 439–453.
- 19 **Honda, H., Nagai, T. and Tanemura, M.** (2008). Two different mechanisms of  
20 planar cell intercalation leading to tissue elongation. *Dev. Dyn.* **237**, 1826–  
21 1836.
- 22 **Hooke, R.** (1665). *Micrographia, or some physiological descriptions of minute*  
23 *bodies made by magnifying glasses, with observations and inquiries*  
24 *thereupon.* London: Royal Society.
- 25 **Huch, M., Knoblich, J. A., Lutolf, M. P. and Martinez-Arias, A.** (2017). The  
26 hope and the hype of organoid research. *Dev.* **144**, 938–941.
- 27 **Inaki, M., Hatori, R., Nakazawa, N., Okumura, T., Ishibashi, T., Kikuta, J.,**  
28 **Ishii, M., Matsuno, K. and Honda, H.** (2018). Chiral cell sliding drives left-  
29 right asymmetric organ twisting. *Elife* **7**, e32506.
- 30 **Inoue, Y., Suzuki, M., Watanabe, T., Yasue, N., Tateo, I., Adachi, T. and**  
31 **Ueno, N.** (2016). Mechanical roles of apical constriction, cell elongation,  
32 and cell migration during neural tube formation in *Xenopus*. *Biomech.*  
33 *Model. Mechanobiol.* **15**, 1733–1746.
- 34 **Inoue, Y., Tateo, I. and Adachi, T.** (2020). Epithelial tissue folding pattern in  
35 confined geometry. *Biomech. Model. Mechanobiol.* **19**, 815–822.
- 36 **Ioannou, F., Dawi, M. A., Tetley, R. J., Mao, Y. and Muñoz, J. J.** (2020).  
37 Development of a New 3D Hybrid Model for Epithelia Morphogenesis.  
38 *Front. Bioeng. Biotechnol.* **8**, 405.
- 39 **Kursawe, J., Bardenet, R., Zartman, J. J., Baker, R. E. and Fletcher, A. G.**  
40 (2016). Robust cell tracking in epithelial tissues through identification of  
41 maximum common subgraphs. *J. R. Soc. Interface* **13**, 20160725.
- 42 **Latorre, E., Kale, S., Casares, L., Gómez-González, M., Uroz, M., Valon, L.,**  
43 **Nair, R. V., Garreta, E., Montserrat, N., del Campo, A., et al.** (2018).  
44 Active superelasticity in three-dimensional epithelia of controlled shape.  
45 *Nature* **563**, 203–208.
- 46 **Lecuit, T. and Lenne, P.-F.** (2007). Cell surface mechanics and the control of  
47 cell shape, tissue patterns and morphogenesis. *Nat. Rev. Mol. Cell Biol.* **8**,  
48 633–644.
- 49 **Lee, C. T., Laughlin, J. G., de la Beaumelle, N. A., Amaro, R. E.,**  
50 **McCammon, J. A., Ramamoorthi, R., Holst, M. and Rangamani, P.**

- 1 (2020). 3D mesh processing using GAMer 2 to enable reaction-diffusion  
2 simulations in realistic cellular geometries. *PLoS Comput. Biol.* **16**,  
3 e1007756.
- 4 **Lewis, F. T.** (1923). The Typical Shape of Polyhedral Cells in Vegetable  
5 Parenchyma and the Restoration of That Shape following Cell Division.  
6 *Proc. Am. Acad. Arts Sci.* **58**, 537–552.
- 7 **Lewis, F. T.** (1925). A Further Study of the Polyhedral Shapes of Cells. *Proc.*  
8 *Am. Acad. Arts Sci.* **61**, 1–34.
- 9 **Lewis, F. T.** (1928). The correlation between cell division and the shapes and  
10 sizes of prismatic cells in the epidermis of cucumis. *Anatom. Rec.* **38**, 341–  
11 376.
- 12 **Lewis, F. T.** (1933). The Significance of Cells as Revealed by Their Polyhedral  
13 Shapes, with Special Reference to Precartilage, and a Surmise concerning  
14 Nerve Cells and Neuroglia. *Proc. Am. Acad. Arts Sci.* **68**, 251–284.
- 15 **Ludwig, H.** (1882). Entwicklungsgeschichte der *Asterina gibbosa* Forbes. *Z.*  
16 *Wiss. Zool* **37**, 1–98.
- 17 **Mao, Y., Tournier, A. L., Bates, P. A., Gale, J. E., Tapon, N. and Thompson,**  
18 **B. J.** (2011). Planar polarization of the atypical myosin Dachs orients cell  
19 divisions in *Drosophila*. *Genes Dev.* **25**, 131–136.
- 20 **Marvin, J. W.** (1939a). The Shape of Compressed Lead Shot and Its Relation  
21 to Cell Shape. *Am. J. Bot.* **26**, 280–288.
- 22 **Marvin, J. W.** (1939b). Cell Shape Studies in the Pith of *Eupatorium*  
23 *purpureum*. *Am. J. Bot.* **26**, 487–504.
- 24 **Menton, D. N.** (1976). A minimum-surface mechanism to account for the  
25 organization of cells into columns in the mammalian epidermis. *Am. J.*  
26 *Anat.* **145**, 1–21.
- 27 **Merzouki, A., Malaspinas, O., Trushko, A., Roux, A. and Chopard, B.**  
28 (2018). Influence of cell mechanics and proliferation on the buckling of  
29 simulated tissues using a vertex model. *Nat. Comput.* **17**, 511–519.
- 30 **Messal, H. A., Alt, S., Ferreira, R. M. M., Gribben, C., Wang, V. M.-Y., Cotoi,**  
31 **C. G., Salbreux, G. and Behrens, A.** (2019). Tissue curvature and  
32 apicobasal mechanical tension imbalance instruct cancer morphogenesis.  
33 *Nature* **566**, 126.
- 34 **Metzcar, J., Wang, Y., Heiland, R. and Macklin, P.** (2019). A Review of Cell-  
35 Based Computational Modeling in Cancer Biology. *JCO Clin. Cancer*  
36 *Informatics* **3**, 1–13.
- 37 **Misra, M., Audoly, B., Kevrekidis, I. G. and Shvartsman, S. Y.** (2016). Shape  
38 Transformations of Epithelial Shells. *Biophys. J.* **110**, 1670–1678.
- 39 **Monier, B., Gettings, M., Gay, G., Mangeat, T., Schott, S., Guarner, A. and**  
40 **Suzanne, M.** (2015). Apico-basal forces exerted by apoptotic cells drive  
41 epithelium folding. *Nature* **518**, 245–248.
- 42 **Mughal, A., Cox, S. J., Weaire, D., Burke, S. R. and Hutzler, S.** (2018).  
43 Demonstration and interpretation of ‘scutoid’ cells formed in a quasi-2D  
44 soap froth. *Philos. Mag. Lett.* **98**, 358–364.
- 45 **Nagai, T. and Honda, H.** (2001). A dynamic cell model for the formation of  
46 epithelial tissues. *Philos. Mag. B* **81**, 699–719.
- 47 **Noll, N., Streichan, S. J. and Shraiman, B. I.** (2020). Variational Method for  
48 Image-Based Inference of Internal Stress in Epithelial Tissues. *Phys. Rev.*  
49 *X* **10**, 011072.
- 50 **Okuda, S., Inoue, Y., Eiraku, M., Adachi, T. and Sasai, Y.** (2015). Vertex

- 1 dynamics simulations of viscosity-dependent deformation during tissue  
2 morphogenesis. *Biomech. Model. Mechanobiol.* **14**, 413–425.
- 3 **Okuda, S., Takata, N., Hasegawa, Y., Kawada, M., Inoue, Y., Adachi, T.,**  
4 **Sasai, Y. and Eiraku, M.** (2018a). Strain-triggered mechanical feedback in  
5 self-organizing optic-cup morphogenesis. *Sci. Adv.* **4**, eaau1354.
- 6 **Okuda, S., Miura, T., Inoue, Y., Adachi, T. and Eiraku, M.** (2018b).  
7 Combining Turing and 3D vertex models reproduces autonomous  
8 multicellular morphogenesis with undulation, tubulation, and branching. *Sci.*  
9 *Rep.* **8**, 2386.
- 10 **Okuda, S., Kuranaga, E. and Sato, K.** (2019). Apical Junctional Fluctuations  
11 Lead to Cell Flow while Maintaining Epithelial Integrity. *Biophys. J.* **116**,  
12 1159–1170.
- 13 **Osterfield, M., Du, X., Schüpbach, T., Wieschaus, E. and Shvartsman, S. Y.**  
14 (2013). Three-Dimensional Epithelial Morphogenesis in the Developing  
15 *Drosophila* Egg. *Dev. Cell* **24**, 400–410.
- 16 **Pearl, E. J., Li, J. and Green, J. B. A.** (2017). Cellular systems for epithelial  
17 invagination. *Philos. Trans. R. Soc. B Biol. Sci.* **372**,.
- 18 **Polyakov, O., He, B., Swan, M., Shaevitz, J. W., Kaschube, M. and**  
19 **Wieschaus, E.** (2014). Passive mechanical forces control cell-shape  
20 change during *drosophila* ventral furrow formation. *Biophys. J.* **107**, 998–  
21 1010.
- 22 **Ramanathan, S. P., Krajnc, M. and Gibson, M. C.** (2019). Cell-Size  
23 Pleomorphism Drives Aberrant Clone Dispersal in Proliferating Epithelia.  
24 *Dev. Cell* **51**, 49-61.e4.
- 25 **Ramón y Cajal, S.** (1888). Sobre las fibras nerviosas de la capa molecular del  
26 cerebelo. *Rev. Trimest. Histol. Norm. y Patológica* 33–49.
- 27 **Ramón y Cajal, S.** (1899). *Textura del sistema nervioso del hombre y de los*  
28 *vertebrados: estudios sobre el plan estructural y composición histológica*  
29 *de los centros nerviosos.* Madrid.
- 30 **Reinhardt, K.** (1918). Über die Zerlegung der Ebene in Polygone.
- 31 **Rivier, N. and Lissowski, A.** (1982). On the correlation between sizes and  
32 shapes of cells in epithelial mosaics. *J. Phys. A. Math. Gen.* **15**, L143–  
33 L148.
- 34 **Robert, A.** (1903). *Recherches sur le développement des troques.* Université  
35 de Paris.
- 36 **Roca-Cusachs, P., Conte, V. and Trepats, X.** (2017). Quantifying forces in cell  
37 biology. *Nat. Cell Biol.* **19**, 742–751.
- 38 **Rossi, G., Manfrin, A. and Lutolf, M. P.** (2018). Progress and potential in  
39 organoid research. *Nat. Rev. Genet.* **19**, 671–687.
- 40 **Rupprecht, J. F., Ong, K. H., Yin, J., Huang, A., Dinh, H. H. Q., Singh, A. P.,**  
41 **Zhang, S., Yu, W. and Saunders, T. E.** (2017). Geometric constraints alter  
42 cell arrangements within curved epithelial tissues. *Mol. Biol. Cell* **28**, 3582–  
43 3594.
- 44 **Sanchez-Corrales, Y. E., Blanchard, G. B. and Röper, K.** (2018). Radially  
45 patterned cell behaviours during tube budding from an epithelium. *Elife* **7**,  
46 e35717.
- 47 **Sanchez-Gutierrez, D., Saez, A., Pascual, A. and Escudero, L. M.** (2013).  
48 Topological progression in proliferating epithelia is driven by a unique  
49 variation in polygon distribution. *PLoS One* **8**, e79227.
- 50 **Sánchez-Gutiérrez, D., Tozluoglu, M., Barry, J. D., Pascual, A., Mao, Y. and**

- 1       **Escudero, L. M.** (2016). Fundamental physical cellular constraints drive  
2       self-organization of tissues. *EMBO J.* **35**, 77–88.
- 3       **Schneider, P. J. and Eberly, D. H.** (2003). *Geometric tools for computer*  
4       *graphics, chapter 10.* Elsevier Science (USA).
- 5       **Sharma, P., Saraswathy, V. M., Xiang, L. and Fürthauer, M.** (2019). Notch-  
6       mediated inhibition of neurogenesis is required for zebrafish spinal cord  
7       morphogenesis. *Sci. Rep.* **9**, 9958.
- 8       **Sharp, T. A., Merkel, M., Manning, M. L. and Liu, A. J.** (2019). Inferring  
9       statistical properties of 3D cell geometry from 2D slices. *PLoS One* **14**,  
10       e0209892.
- 11       **Spangenberg, F.** (1875). Zur Kenntnis von Branchipus stagnalis. *Zeit. f. wiss.*  
12       *Zool. Bd* **25**, 1–64.
- 13       **Staddon, M. F., Bi, D., Tabatabai, A. P., Ajeti, V., Murrell, M. P. and**  
14       **Banerjee, S.** (2018). Cooperation of dual modes of cell motility promotes  
15       epithelial stress relaxation to accelerate wound healing. *PLOS Comput.*  
16       *Biol.* **14**, e1006502.
- 17       **Staddon, M. F., Cavanaugh, K. E., Munro, E. M., Gardel, M. L. and**  
18       **Banerjee, S.** (2019). Mechanosensitive Junction Remodeling Promotes  
19       Robust Epithelial Morphogenesis. *Biophys. J.* **117**, 1739–1750.
- 20       **Sugimura, K., Lenne, P.-F. F. and Graner, F.** (2016). Measuring forces and  
21       stresses in situ in living tissues. *Development* **143**, 186–196.
- 22       **Sui, L., Alt, S., Weigert, M., Dye, N., Eaton, S., Jug, F., Myers, E. W.,**  
23       **Jülicher, F., Salbreux, G. and Dahmann, C.** (2018). Differential lateral  
24       and basal tension drive folding of Drosophila wing discs through two  
25       distinct mechanisms. *Nat. Commun.* **9**, 4620.
- 26       **Sun, Z., Amourda, C., Shagirov, M., Hara, Y., Saunders, T. E. and Toyama,**  
27       **Y.** (2017). Basolateral protrusion and apical contraction cooperatively drive  
28       Drosophila germ-band extension. *Nat. Cell Biol.* **19**, 375–383.
- 29       **Tetley, R. J., Staddon, M. F., Heller, D., Hoppe, A., Banerjee, S. and Mao, Y.**  
30       (2019). Tissue fluidity promotes epithelial wound healing. *Nat. Phys.* **15**,  
31       1195–1203.
- 32       **Thompson, D. W. D.** (1917). *On growth and form.* Cambridge university press.
- 33       **Thomson, W.** (1887). LXIII. On the division of space with minimum partitional  
34       area. *London, Edinburgh, Dublin Philos. Mag. J. Sci.* **24**, 503–514.
- 35       **Tsuboi, A., Ohsawa, S., Umetsu, D., Sando, Y., Kuranaga, E., Igaki, T. and**  
36       **Fujimoto, K.** (2018). Competition for Space Is Controlled by Apoptosis-  
37       Induced Change of Local Epithelial Topology. *Curr. Biol.* **28**, 2115–2128.
- 38       **Tuveson, D. and Clevers, H.** (2019). Cancer modeling meets human organoid  
39       technology. *Science (80- )*. **364**, 952–955.
- 40       **Vasan, R., Maleckar, M. M., Williams, C. D. and Rangamani, P.** (2019).  
41       DLITE Uses Cell-Cell Interface Movement to Better Infer Cell-Cell  
42       Tensions. *Biophys. J.* **117**, 1714–1727.
- 43       **Veldhuis, J. H., Ehsandar, A., Maître, J.-L., Hiiragi, T., Cox, S. and**  
44       **Brodland, G. W.** (2017). Inferring cellular forces from image stacks. *Philos.*  
45       *Trans. R. Soc. B Biol. Sci.* **372**, 20160261.
- 46       **Vicente-Munuera, P., Gómez-Gálvez, P., Tetley, R. J., Forja, C., Tagua, A.,**  
47       **Letrán, M., Tozluoglu, M., Mao, Y. and Escudero, L. M.** (2020).  
48       EpiGraph: an open-source platform to quantify epithelial organization.  
49       *Bioinformatics* **36**, 1314–1316.
- 50       **Wetzel, G.** (1926). Zur entwicklungsmechanischen Analyse des einfachen

1       prismatischen Epithels. *Wilhelm Roux Arch. für Entwicklungsmechanik der*  
2       *Org.* **107**, 177–185.

3       **Wolny, A., Cerrone, L., Vijayan, A., Tofanelli, R., Barro, A. V., Louveaux, M.,**  
4       **Wenzl, C., Strauss, S., Wilson-Sánchez, D., Lymbouridou, R., et al.**  
5       (2020). Accurate and versatile 3D segmentation of plant tissues at cellular  
6       resolution. *Elife* **9**, 1–34.

7       **Xu, B., Washington, A. M., Domeniconi, R. F., Ferreira Souza, A. C., Lu, X.,**  
8       **Sutherland, A. and Hinton, B. T.** (2016). Protein tyrosine kinase 7 is  
9       essential for tubular morphogenesis of the Wolffian duct. *Dev. Biol.* **412**,  
10       219–233.

11       **Xu, M., Wu, Y., Shroff, H., Wu, M. and Mani, M.** (2018). A scheme for 3-  
12       dimensional morphological reconstruction and force inference in the early  
13       c. *Elegans* embryo. *PLoS One* **13**, e0199151.

14       **Yamashita, S. and Michiue, T.** (2014). Quantitative analysis of cell  
15       arrangement indicates early differentiation of the neural region during  
16       *Xenopus* gastrulation. *J. Theor. Biol.* **346**, 1–7.

17       **Yin, X., Mead, B. E., Safaei, H., Langer, R., Karp, J. M. and Levy, O.** (2016).  
18       Engineering Stem Cell Organoids. *Cell Stem Cell* **18**, 25–38.

19       **Yokouchi, M., Atsugi, T., Van Logtestijn, M., Tanaka, R. J., Kajimura, M.,**  
20       **Suematsu, M., Furuse, M., Amagai, M. and Kubo, A.** (2016). Epidermal  
21       cell turnover across tight junctions based on Kelvin’s tetrakaidecahedron  
22       cell shape. *Elife* **5**, e19593.

23       **Zhu, H. X., Thorpe, S. M. and Windle, A. H.** (2001). The geometrical  
24       properties of irregular two-dimensional Voronoi tessellations. *Philos. Mag.*  
25       **A 81**, 2765–2783.

26  
27  
28

## 1 Glossary

2

3 **Aboav-Weaire's law:** It establishes that, in the surface of an epithelium, cells  
4 with a larger number of sides tend to have cell neighbours with few sides, and  
5 vice versa.

6 **Apico-basal intercalation:** Cells rearrangement along the apico-basal axis in  
7 which the cells exchange their neighbours between the basal and the apical  
8 surfaces. Roughly speaking an apico-basal intercalation is similar to a T1  
9 transition, but the neighbour exchange between cells occurs in space (along the  
10 apico-basal cell axis) instead of as a function of time.

11 **Euler's principle:** The Euler formula relates the number of vertices (V), edges  
12 (E) and faces (F) of polygons with the so-called Euler characteristic (2 in convex  
13 tessellations of the plane):  $V - E + F = 2$ .

14 **Flintstones' law:** It states that the average number of 3D connections of cells  
15 of monolayer tubular epithelia grows as a function of the surface ratio (apico-  
16 basal coordinate) following a logistic-like formula.

17 **Graph Theory:** Branch of mathematics that focuses on the study of network  
18 properties. Typically, a network is constituted by a set of nodes connected by  
19 edges, and these pairwise relationships are the object of analysis.

20 **Lewis' law:** It states that, in the surface of an epithelium, the fractional apical  
21 cell area increases linearly with the number of neighbours of a cell (so, small  
22 cells tend to have less sides than larger cells).

23 **Vertex models:** Off-lattice tissue simulation scheme based on the balance of  
24 forces acting on a limited set of points that describe every cell: the vertices that  
25 define their polygonal shape.

26 **Voronoi tessellations:** Mathematical concept based on compartmentalizing  
27 the Euclidean space by proximity, in which, each one of the compartments is  
28 called Voronoi cell. For developing a Voronoi diagram is necessary a set of  
29 seeds. From each seed will emerge a Voronoi cell filling the surface preventing  
30 gaps among the cells, and not allowing overlapping between the regions,  
31 resulting in a subdivision of convex polygons that follow the rule that a Voronoi



1 cell contains all the points of space that are closer to its seed than any other  
2 seed.

3 **Young-Laplace formula/equation:** Given a thin interface that separates two  
4 fluids, the Young-Laplace formula evaluates the balance of normal stresses  
5 acting on the interface (i.e. surface) and relates the pressure differences with  
6 the surface tension and the local geometry (principal curvatures).

7

8

9

10

11

## 12 **Funding**

13

14 L.M.E, P.V.-M. and P.G.-G. has been supported by the Ramón y Cajal program  
15 (PI13/01347); L.M.E, P.V.-M. and P.G.-G. work is funded by the Ministry of  
16 Economy, Industry and Competitiveness grant BFU2016-74975-P and Spanish  
17 Ministry of Science and Innovation grant PID2019-103900GB-I00 co-funded by  
18 FEDER funds. L.M.E also acknowledges financial support from the Andalusian  
19 government Consejería de Economía, Innovación y Ciencia through grant P18-  
20 FR-631 co-funded by FEDER funds. S.A. and J.B. have been supported by a  
21 Faculty Innovation Grant (FIG) by Lehigh University JB-FIG-2019. J.B. also  
22 acknowledges financial support from the Spanish Ministry of Science and  
23 Innovation through grant 2019-105566GB-I00.

24

1 **Fig. 1. Schematic representation of monolayer epithelial tissues. (A)**  
2 Illustration of a planar epithelium where cells are represented as prismatic  
3 columns. **(B)** Cells in (A) adapt their conformation to the tissue curvature by  
4 adopting the shape of a truncated pyramid (i.e. frustum). **(C)** A Voronoi tubular  
5 model mimicking a monolayer epithelial tube, where some cells have been  
6 peeled-off (from left to right) to reveal their three-dimensional arrangement. The  
7 four-cell motif formed by the blue, red, green and yellow cells undergoes an  
8 apico-basal intercalation (spatial T1 transition). Red and green cells in contact  
9 at the basal surface (outer surface), but they are not at the apical surface (inner  
10 surface). The opposite happens with blue and yellow cells: they are neighbours  
11 in the apical surface but not in the basal surface. All four cells have scutoidal  
12 shapes. The colours of the cells in (A) and (B) are consistent to track the  
13 changes that occur during the transition from a planar to a bent tissue. In the  
14 center and right panels in (C) the cells that do not belong to the four-cell motif  
15 have been shaded to highlight the cells with a scutoidal shape.

16

17 **Fig 2. Historical timeline summarizing breakthroughs in the**  
18 **characterization of 3D cell shapes and their arrangements.** A timeline of  
19 different realistic descriptions of cell shapes. Yellow-golden colours highlight  
20 studies related to solids with 14 faces. The grey-blue-pink colours highlight  
21 studies connected to the existence of apico-basal cell intercalations in  
22 monolayer epithelia. In 1887, Lord Kelvin proposed the geometrical shape of a  
23 'orthic tetrakaidekahedrum' as a theoretical solution to fill the space optimally. In  
24 1925, Lewis confirmed the existence of tetrakaidecahedra cells, also found by  
25 Menton as predominant on the epidermal tissue. In 2016, Yokouchi and  
26 colleagues supported Lord Kelvin's tetrakaidekahedrum as a cellular shape,  
27 revealing its predominance and important role in stratified epithelia. In a  
28 different context, in 1903, Robert found early scutoidal-like cellular  
29 configurations later revisited by, D'Arcy Thompson in 1917, highlighting its  
30 importance. In 1991, Condic and colleagues challenged the 'prismatic  
31 approximation' by showing that the cellular organization at the apical and basal  
32 layers of an epithelium changed during *Drosophila* development, suggesting the  
33 existence of apico-basal intercalations. These intercalations were theoretically  
34 postulated by Honda and colleagues as transient cellular configurations to

1 achieve tissue elongation, and were later envisioned as cellular protrusions by  
2 Sun and colleagues during *Drosophila's* germ-band extension. Recently, two  
3 studies emphasized the role of T1-spatial transitions or interleaving in different  
4 contexts of developmental biology: in 2018, Gómez-Gálvez and colleagues  
5 formally proposed that the spatial intercalations entailed a new cell shape  
6 (scutoid) that develops as a consequence of biophysical and geometrical  
7 constraints, which were confirmed in a study using soap bubbles.

8

9 **Fig 3. Mathematical approaches towards the analysis of epithelia.** The  
10 analysis of epithelia from the perspective of space tessellations using convex  
11 polygons has led to a number of quantitative laws in morphogenesis. **(A)** Euler's  
12 principle for convex polyhedra implies that Vertex ( $V$ ) - Edges ( $E$ ) + Faces ( $F$ ) =  
13 2. In this figure the labels inside the polygons indicate their number of vertices  
14 or edges,  $n$ . In this case,  $V=13$ ,  $E=15$ , and  $F=4$  (note that the external face  
15 surrounding all polygons is also included in the face count). **(B)** Euler's formula  
16 implies that in the thermodynamic limit, that is, as the number of cells becomes  
17 very large, the average number of neighbours (edges) if a cell in 2D, i.e.  $\langle n \rangle$ ,  
18 approaches six. **(C)** By denoting by  $\langle A \rangle_n$  the average area of cells with  $n$   
19 number of edges and by  $\langle A \rangle$  the average cell area, Lewis' law states that the  
20 fractional area of cells,  $\langle A \rangle_n / \langle A \rangle$ , that belong to a polygonal class (i.e. triangles,  
21 squares, pentagons...) increases linearly with the polygonal class (i.e. with  $n$ ).  
22 Lewis' law is a consequence of a maximum entropy principle and cellular  
23 topological constraints. **(D)** On the other hand, Aboav-Weaire's law provides an  
24 analytical dependence of the average number of neighbours of neighbouring  
25 cells on the polygonal class. Thus,  $\langle m \rangle_n$  indicates the average number of edges  
26 of cells that are neighbour with a cell with  $n$  edges: the larger the polygonal  
27 class,  $n$ , the smaller the number of edges of neighbouring cells. **(E)** Gibson and  
28 colleagues later established the universality of the polygonal distribution of cells  
29 due to division events. In agreement with Euler's formula the average of this  
30 distribution is 6. **(F)** More recently, laws are being proposed in the context of the  
31 3D shape of cells. In particular, the Flintstone's law states that, as a function of  
32 the so-called surface ratio,  $R_b/R_a$ , tubular epithelia increase their 3D

1 connectivity (i.e. the 3D number of neighbours) in a logistic manner as a  
2 consequence of apico-basal intercalations.

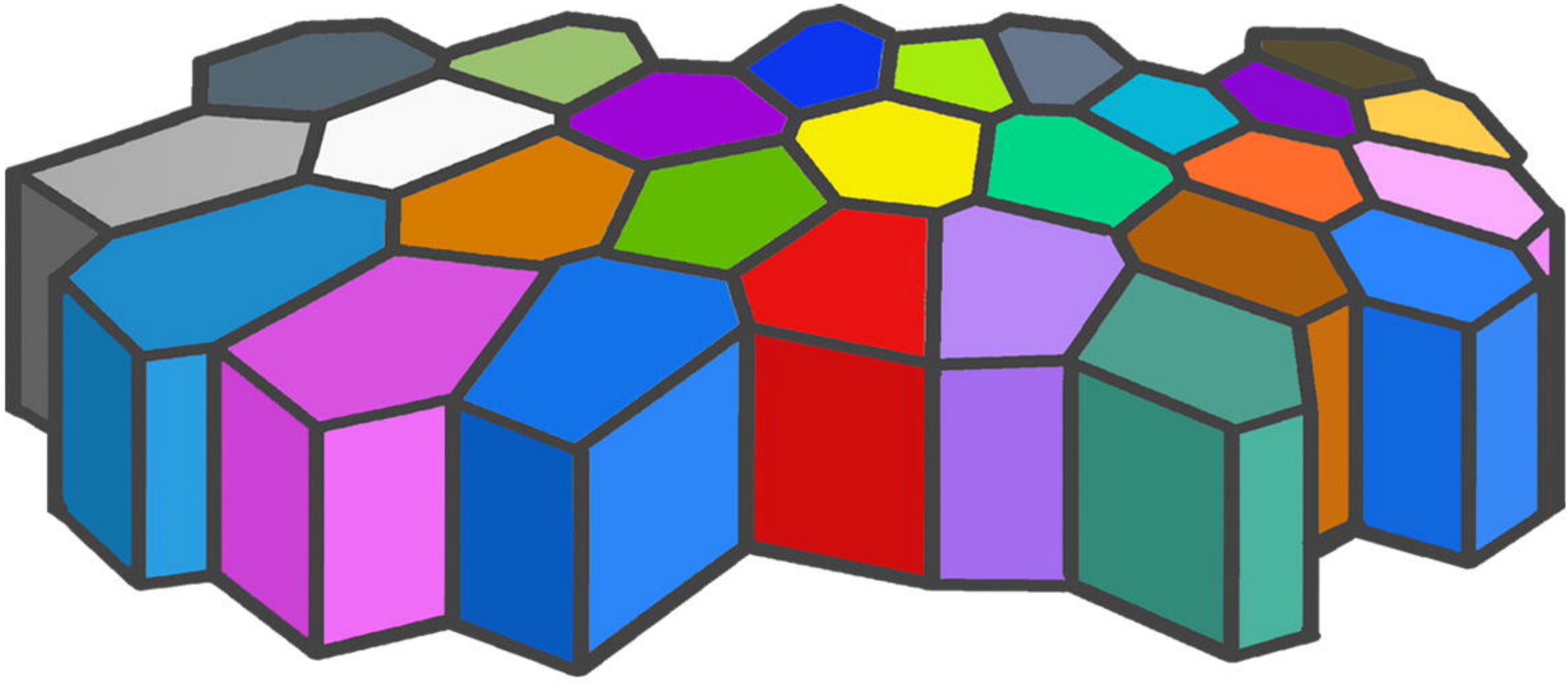
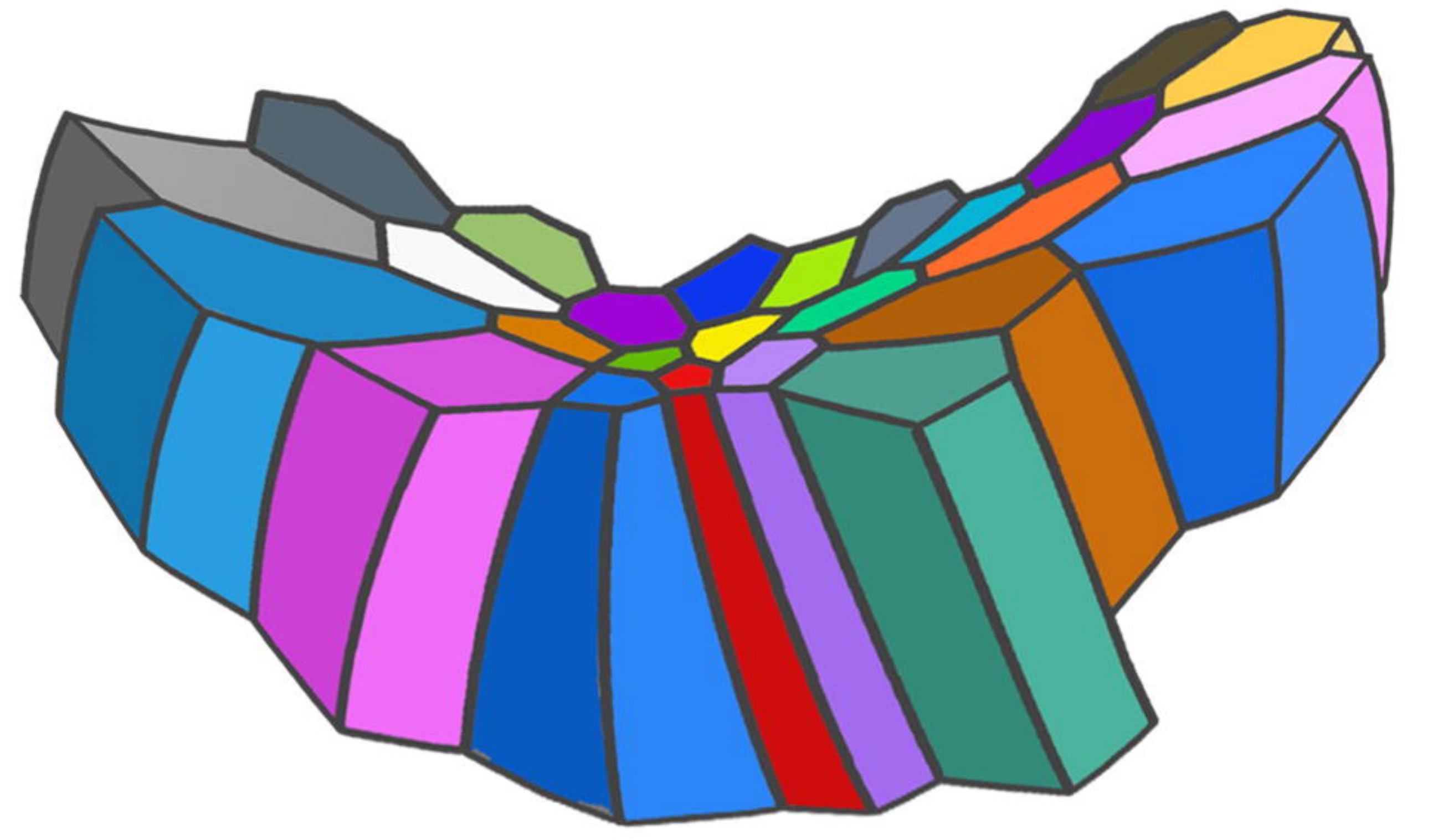
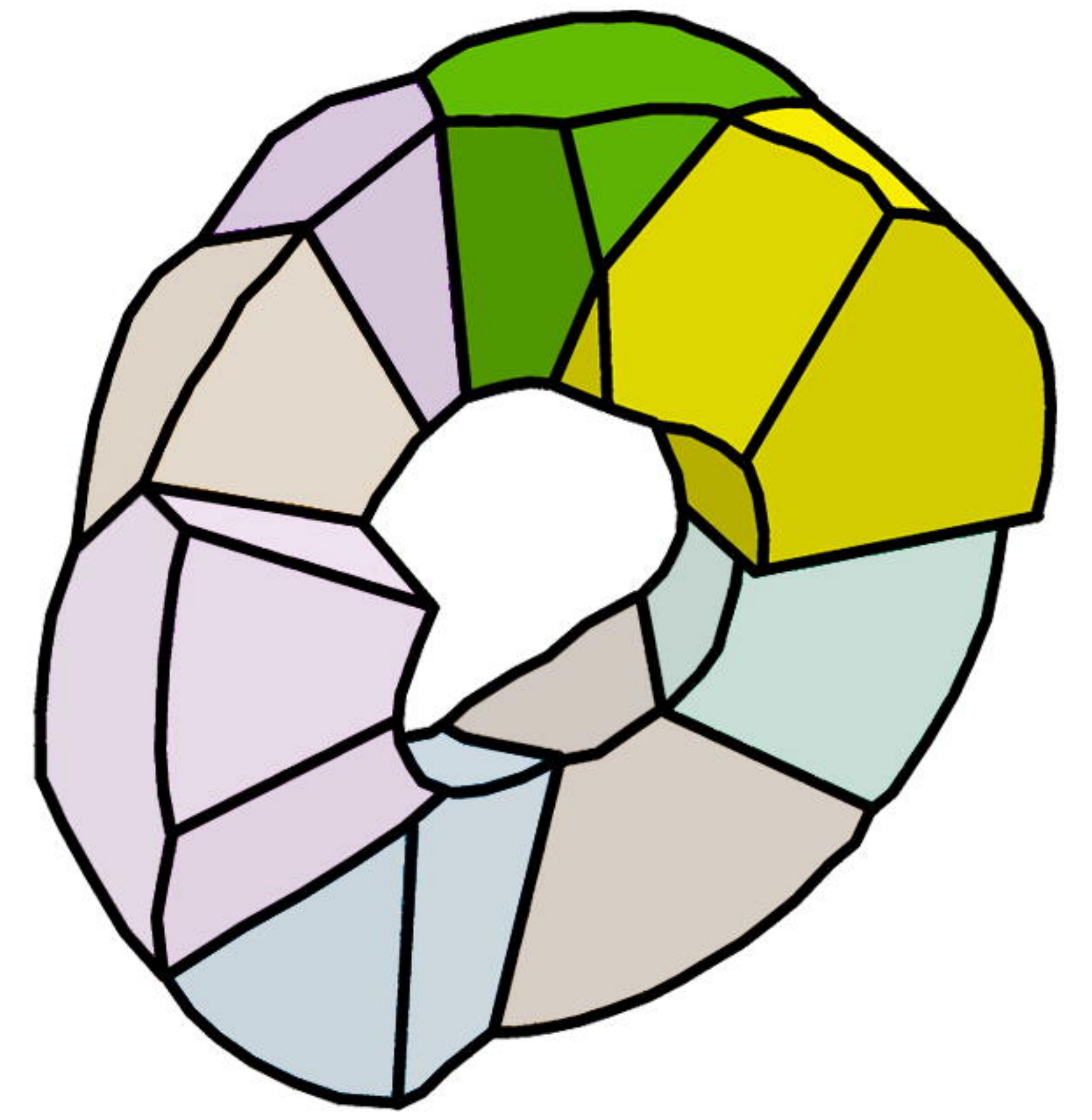
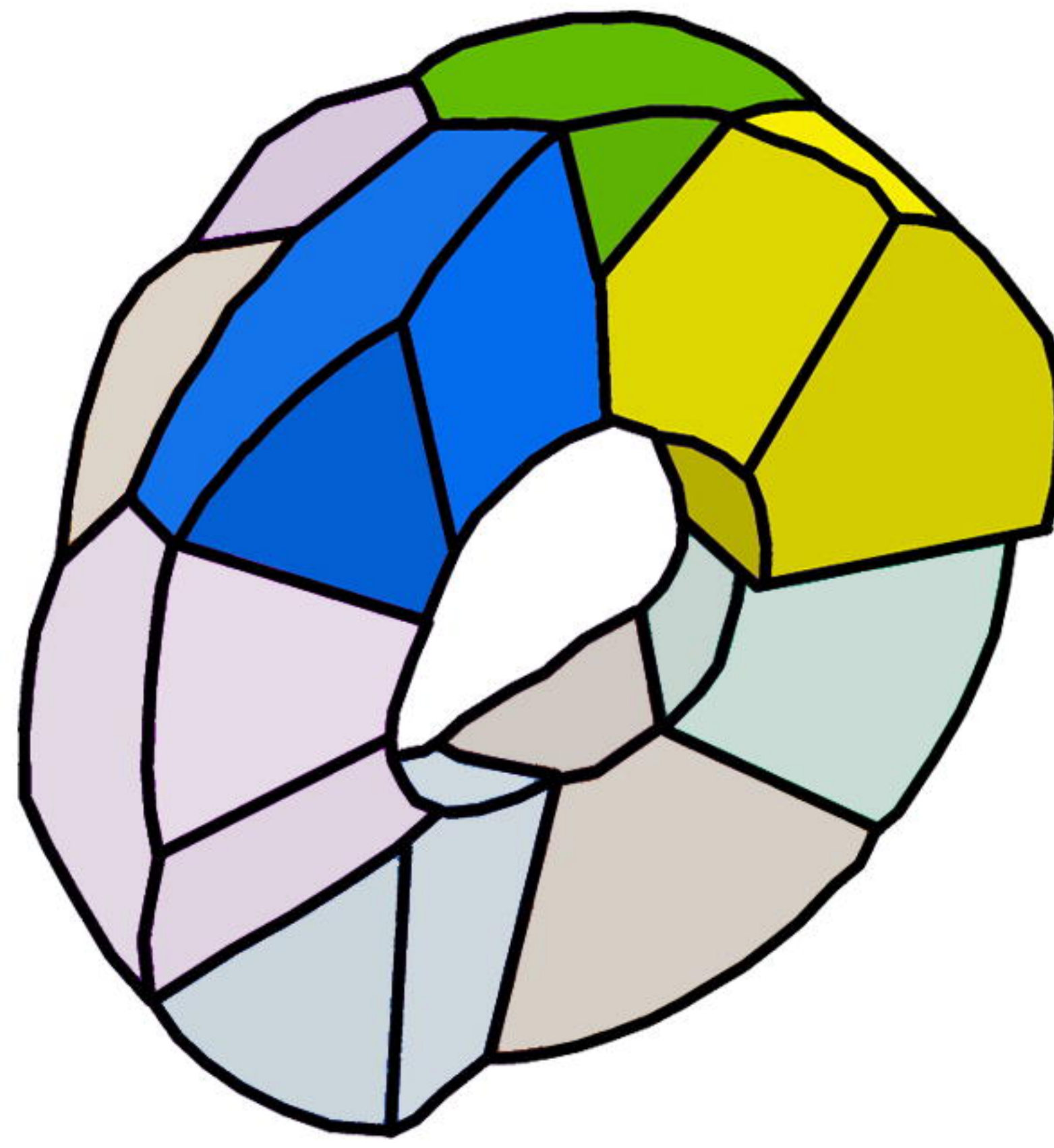
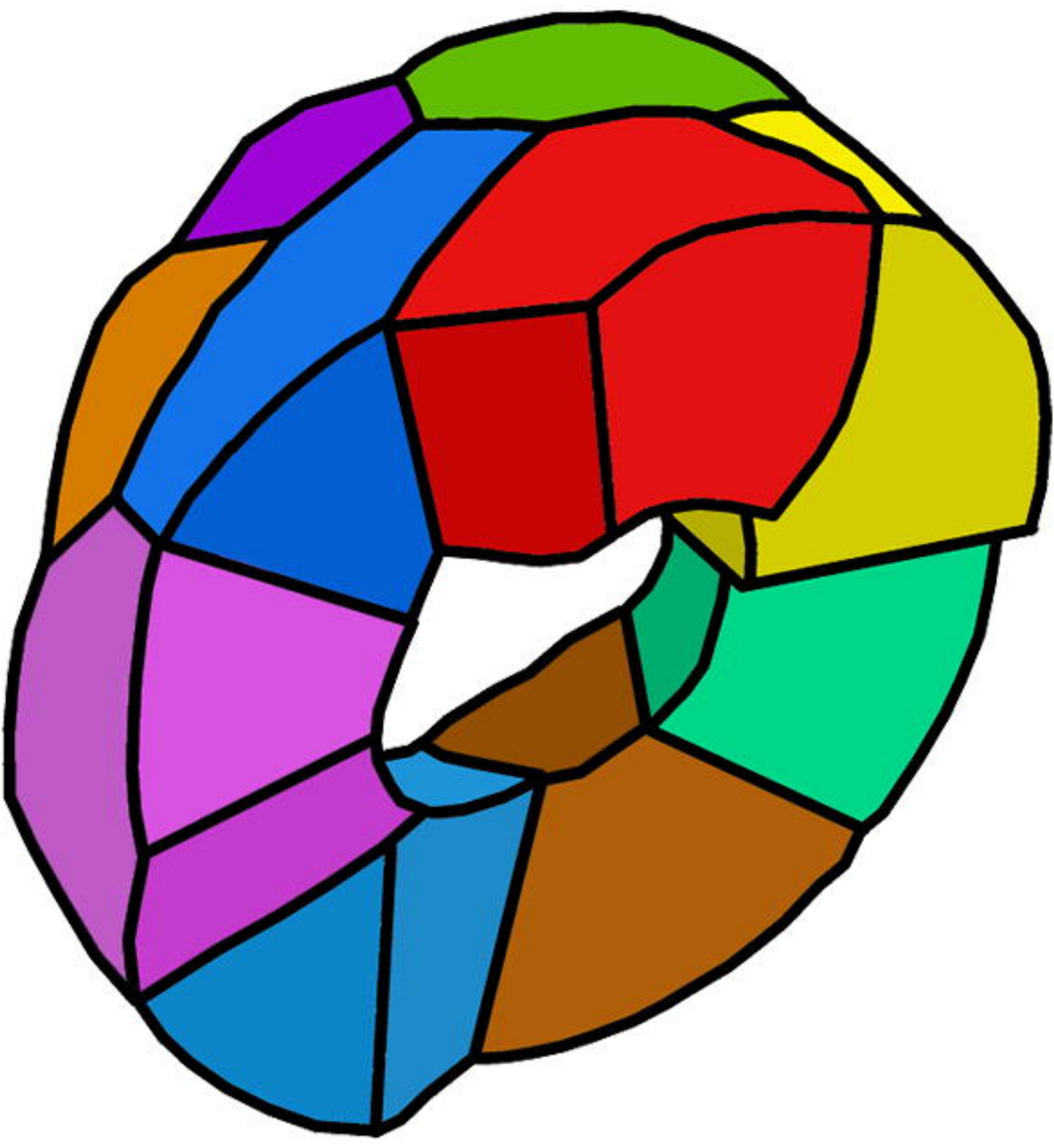
3

4 **Fig. 4. Non-invasive force inference methods.** (A) Force inference methods  
5 based on the geometrical analysis of cellular arrangements ultimately rely on  
6 applications of a force equilibrium principle on the cellular vertices (top) and/or  
7 on the Laplace-Young law (bottom). As for the former, the equilibrium of forces  
8 at cell junctions (vertices) implies a balance between pressure terms,  $P$ , and  
9 membrane tensions,  $T$ . That hypothesis leads to the estimation of parameters  
10 ( $A$  and  $B$  in this panel), that measure the relative pressure/tension force  
11 contributions. On the other hand, the methodology based on the Laplace-Young  
12 law is based on the assumption that cells behave mechanically as fluid objects.  
13 Thus, it relates the cellular, or the tissue-level, membrane tension,  $\sigma$ , the acting  
14 normal stresses,  $\Delta P$ , that modulate the cell (tissue) shape, and the principal  
15 curvatures at a given location,  $1/R_1$  and  $1/R_2$ , that define the local geometry.  
16 (B) On the modelling side, the vertex model has successfully reproduced a  
17 number of morphogenetic processes. The canonical form of the vertex model  
18 includes mechanical contributions at cell vertices due to a) the area,  $A$ , that  
19 leads to spring-like forces (volume conservation), b) the action of the  
20 actomyosin ring along the cell perimeter,  $L$ , that simulate contractile effects, and  
21 adhesion terms that mimics membrane tension along cell contacts,  $l$ . By  
22 including non-equilibrium effects, such as cell growth and division, and  
23 assuming a fast balance of the mechanical forces, the position of cell vertices  
24 can be tracked in space and time and hence the cellular motion. Current  
25 challenges in the field of epithelial tissue simulation schemes include the  
26 development of techniques that reproduce realistically the 3D arrangements of  
27 cells and clarify the driving forces underlying apico-basal intercalations.

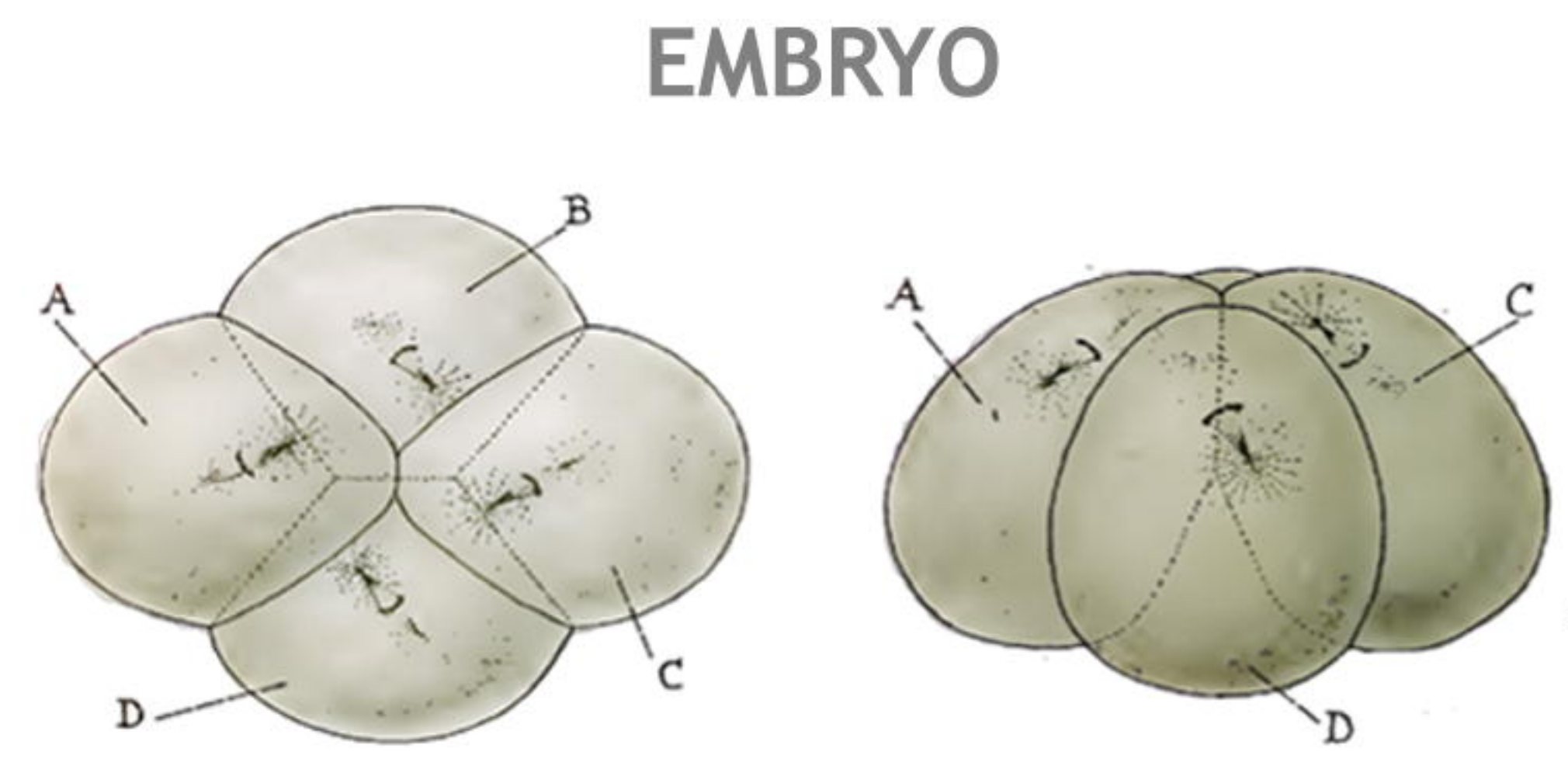
28

29



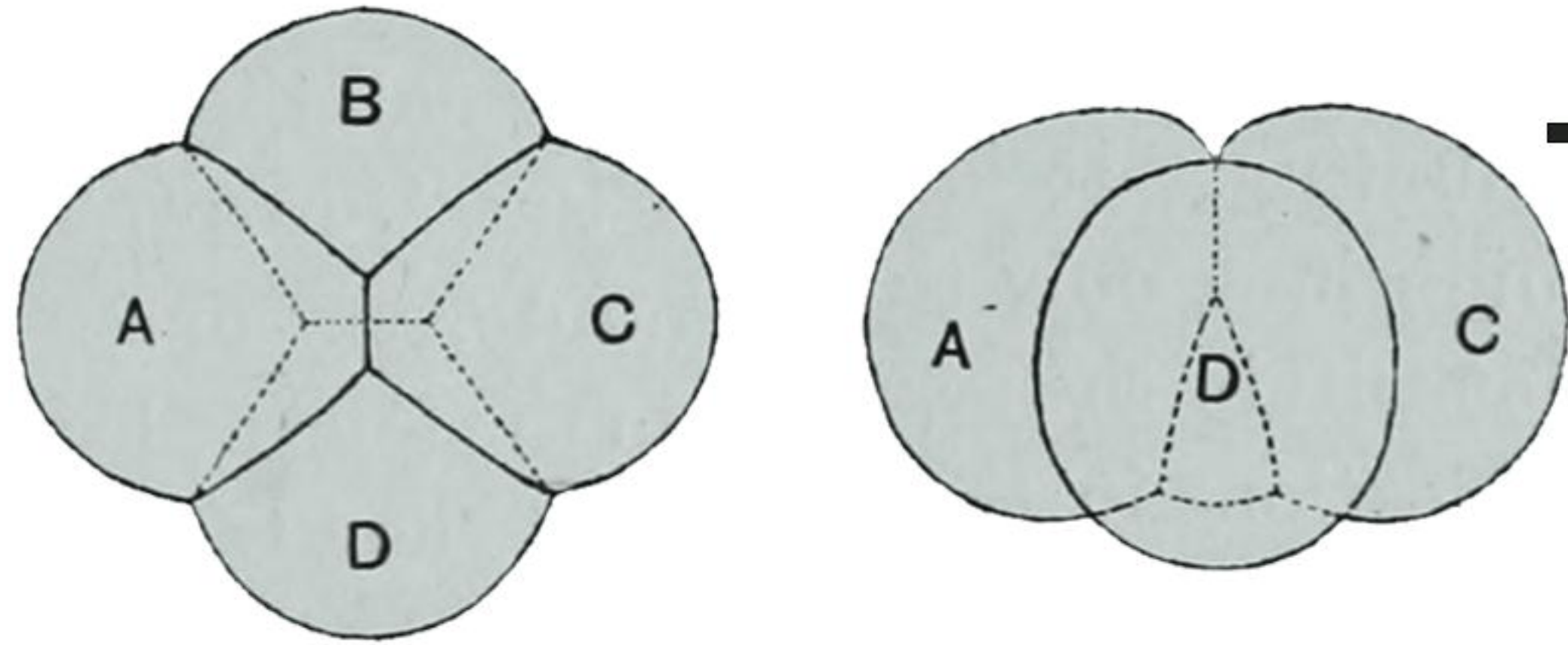
**A****B****C**



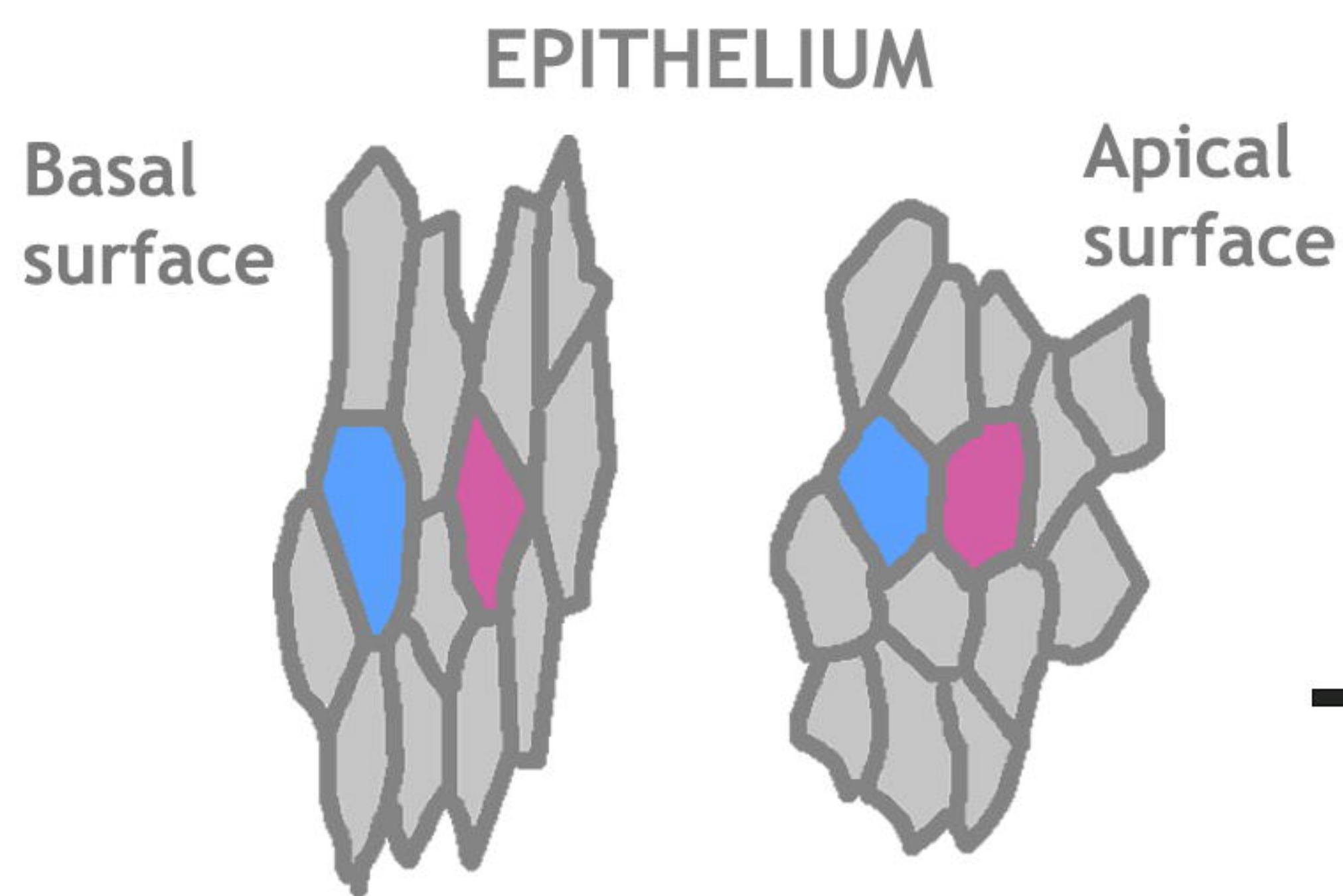


EMBRYO

Robert, 1903



Thompson, 1917

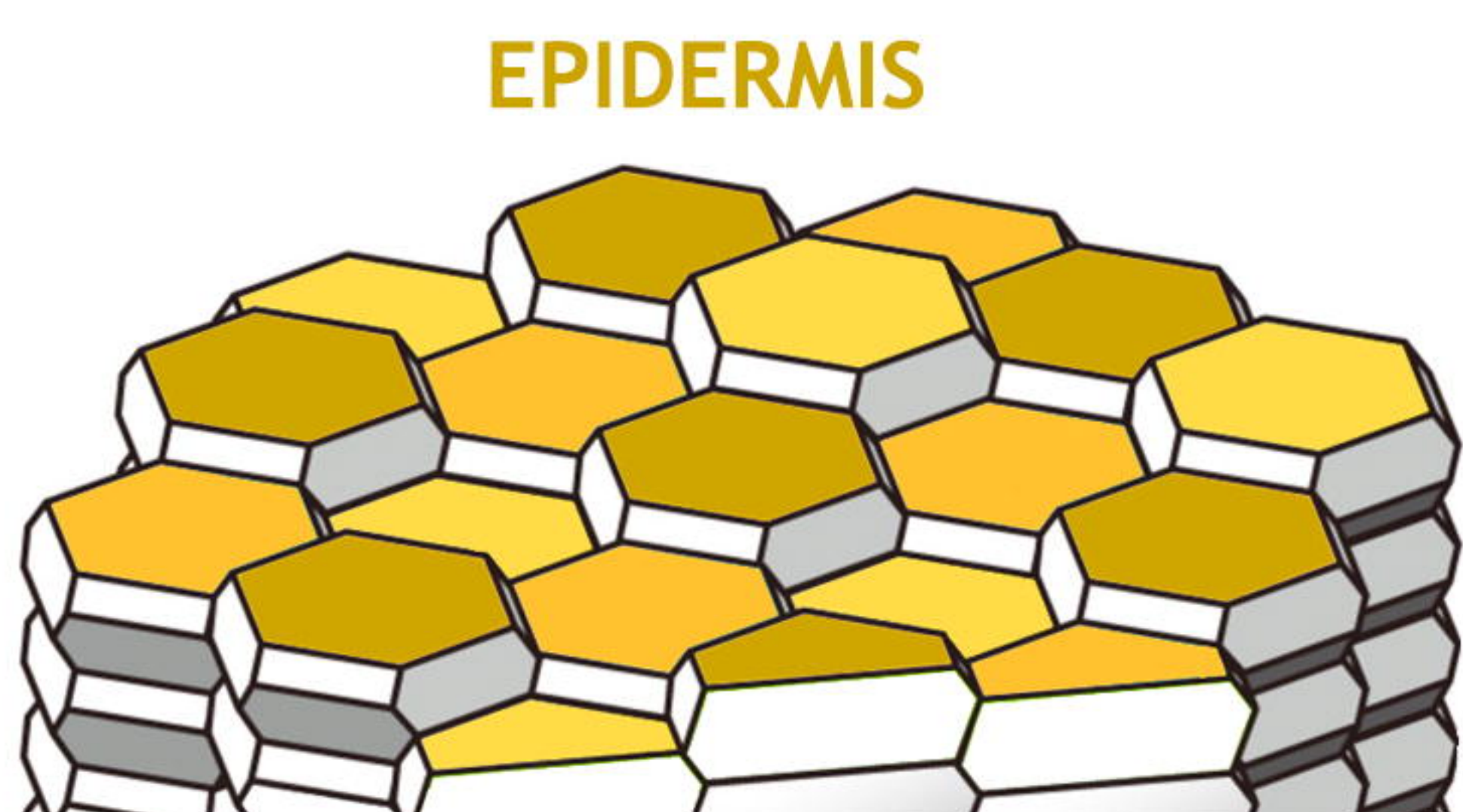


EPITHELIUM

Basal surface

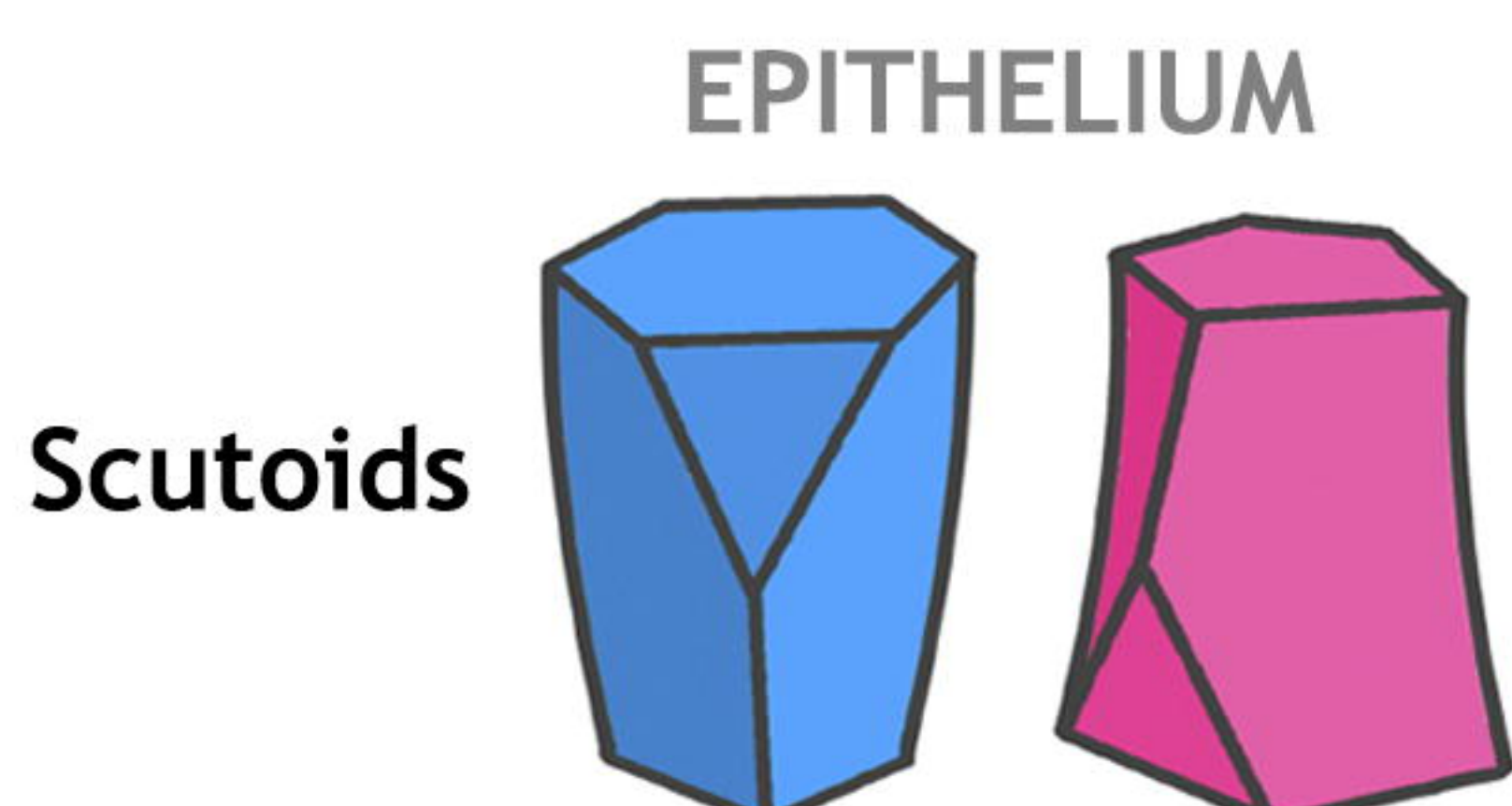
Apical surface

Condic et al., 1991  
Xu et al., 2016



EPIDERMIS

Yokouchi et al., 2016

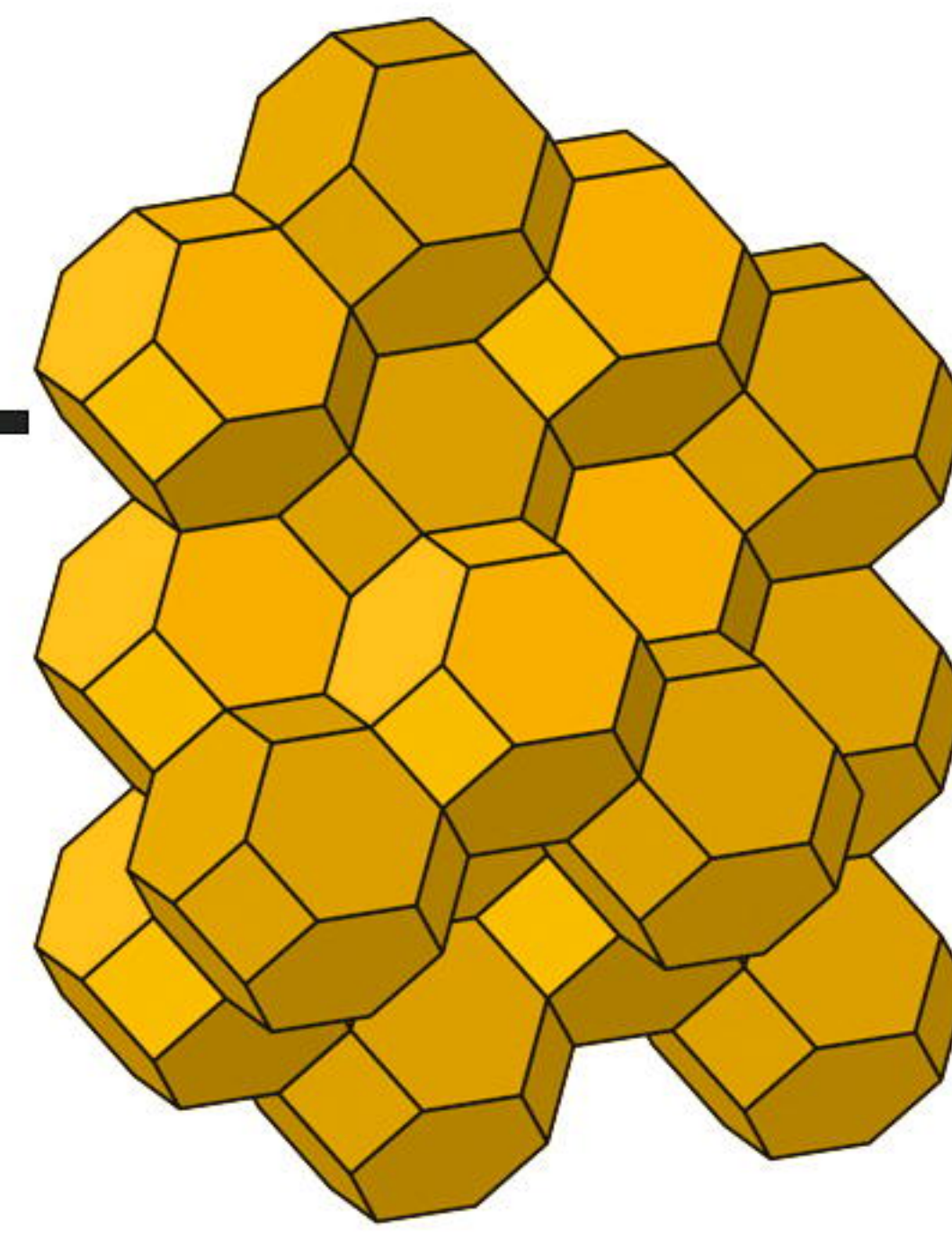


EPITHELIUM

Scutoids

Gómez-Gálvez et al., 2018  
Mughal et al., 2018

1887



Orthic tetrakaidecahedra

1903

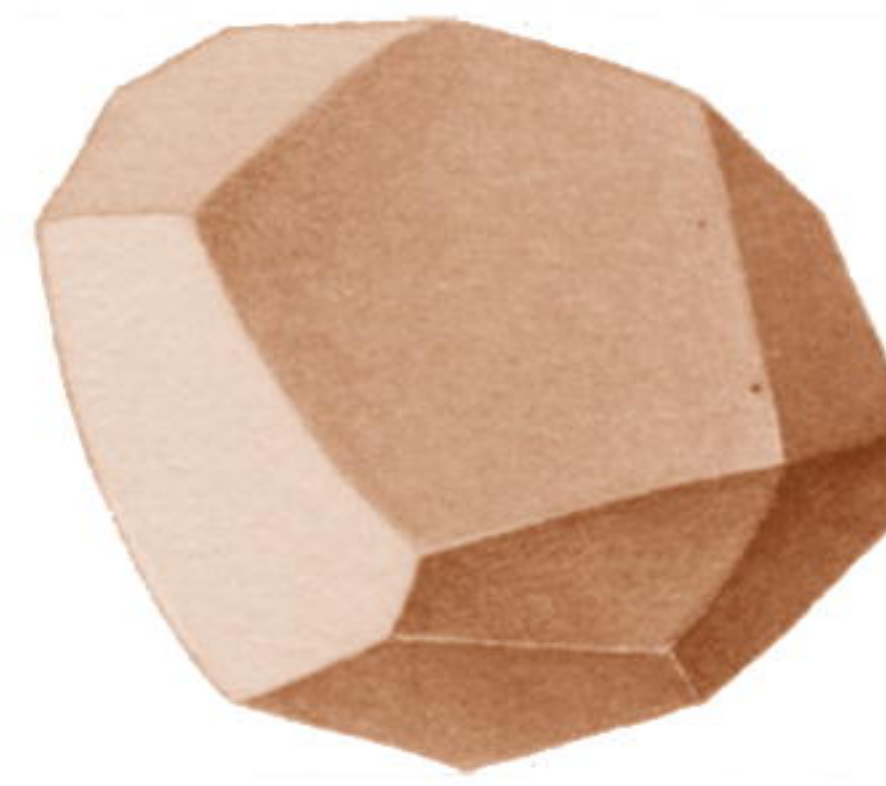
Lord Kelvin, 1887

1917

1925

FAT TISSUE

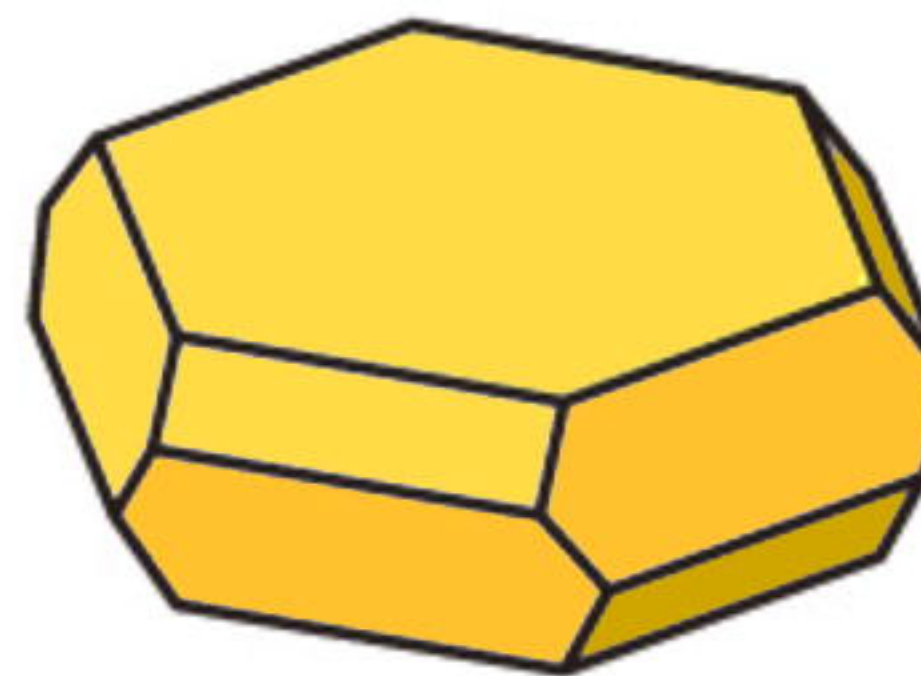
Tetrakaidecahedrum



Lewis et al., 1925

EPIDERMIS

Flatten tetrakaidecahedrum

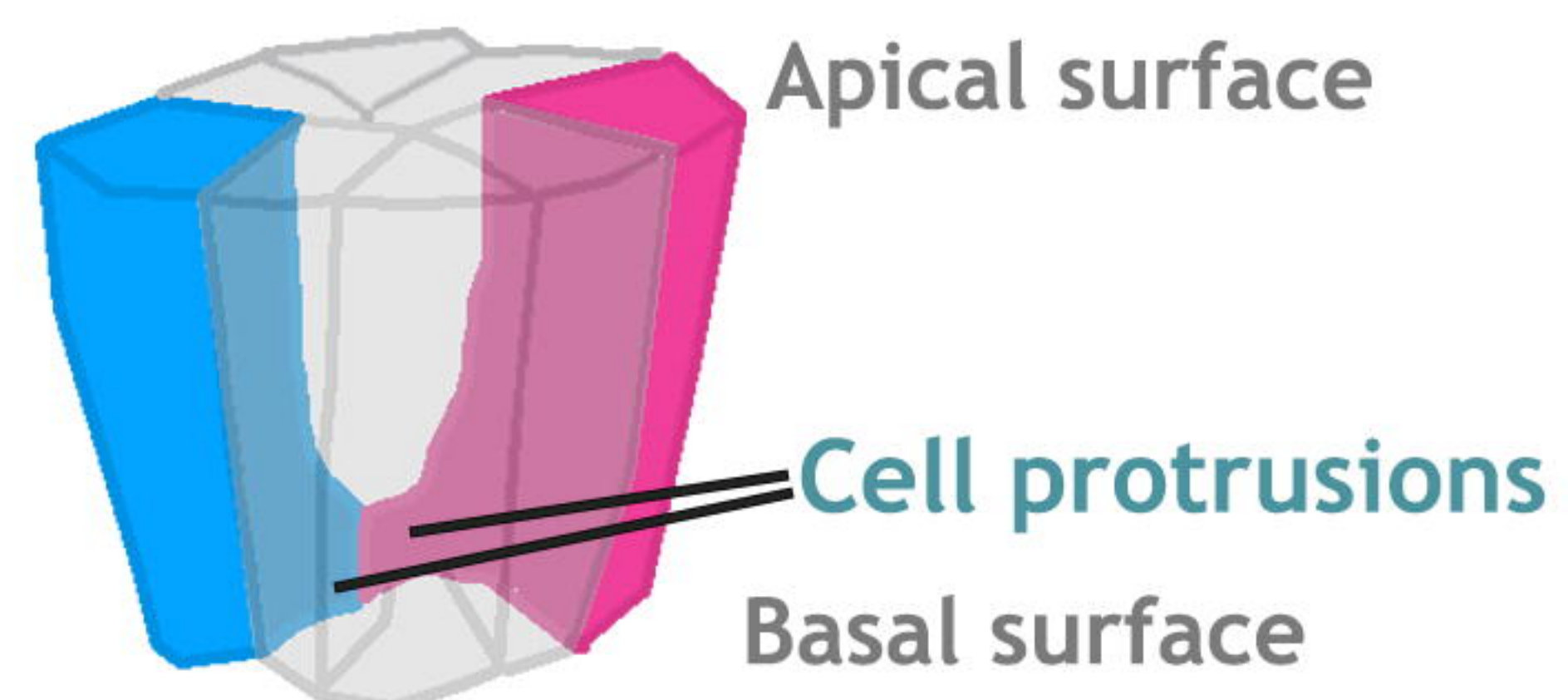


1976

Allen and Potten, 1976  
Menton, 1976

1991

EPITHELIUM



Honda et al., 2008  
Sun et al., 2017

2008

2016

EPITHELIUM



2017



2018

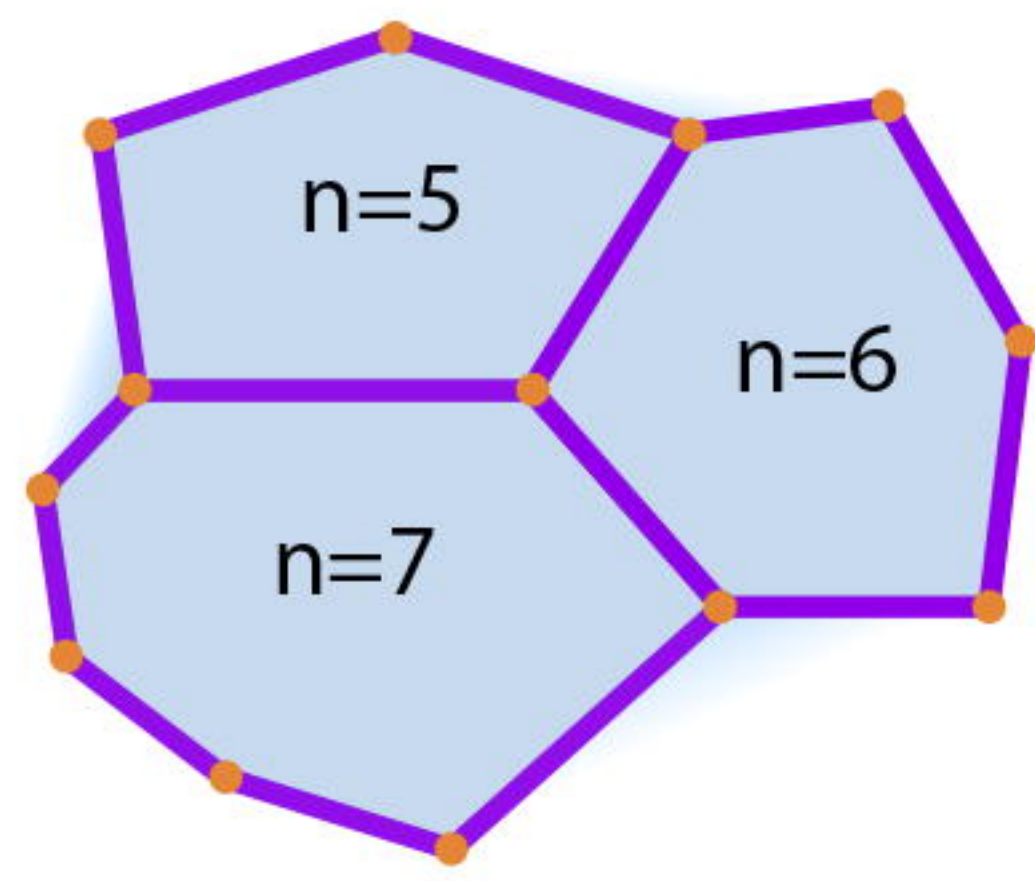


Rupprecht et al., 2017  
Sánchez-Corrales, et al. 2018

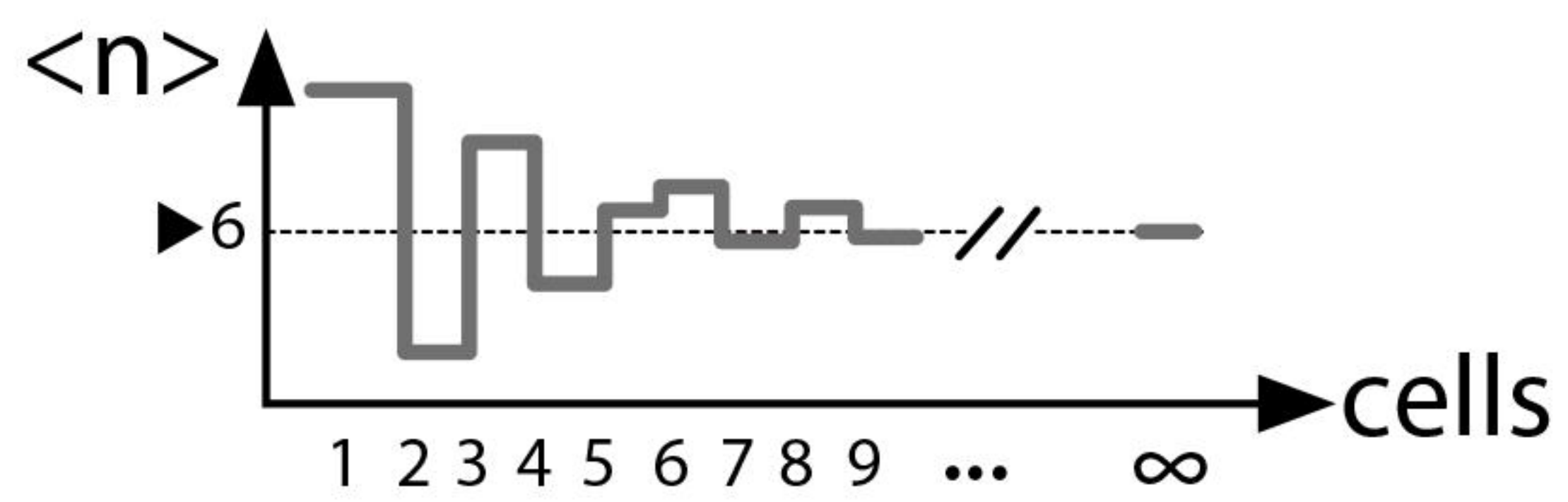


**A**

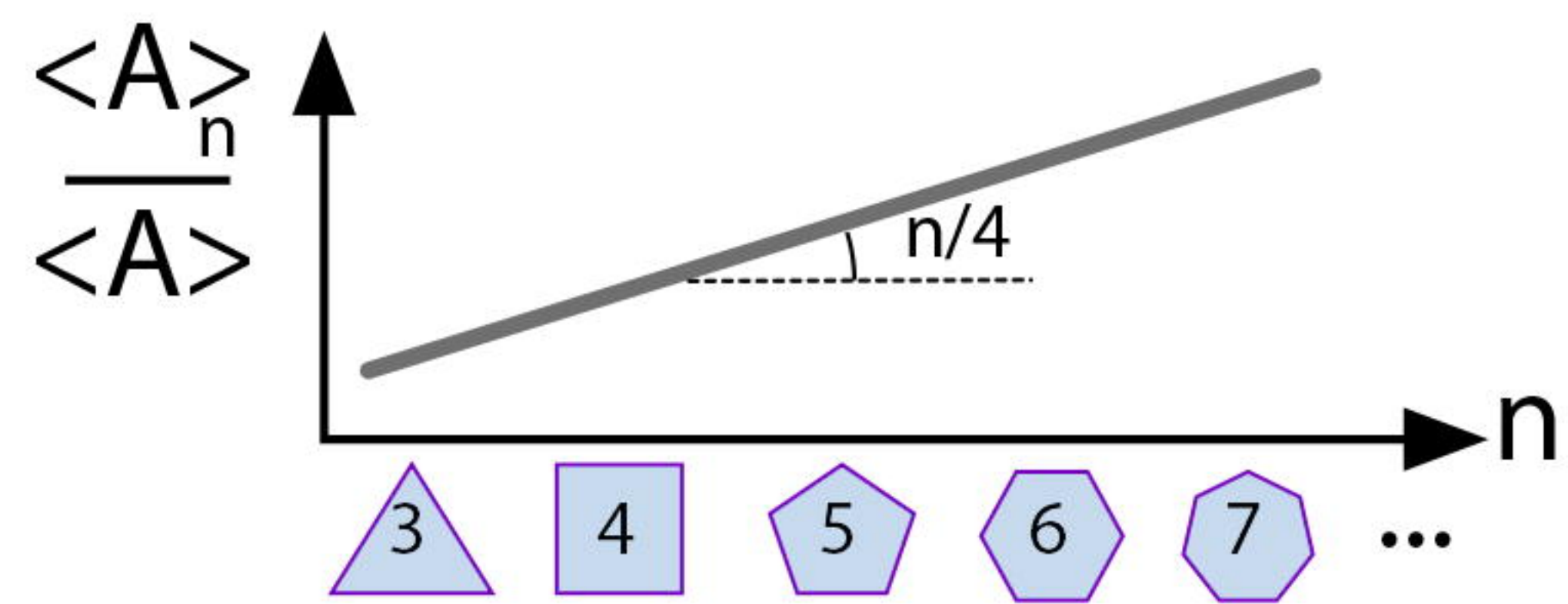
$$V - E + F = 2$$

**B**

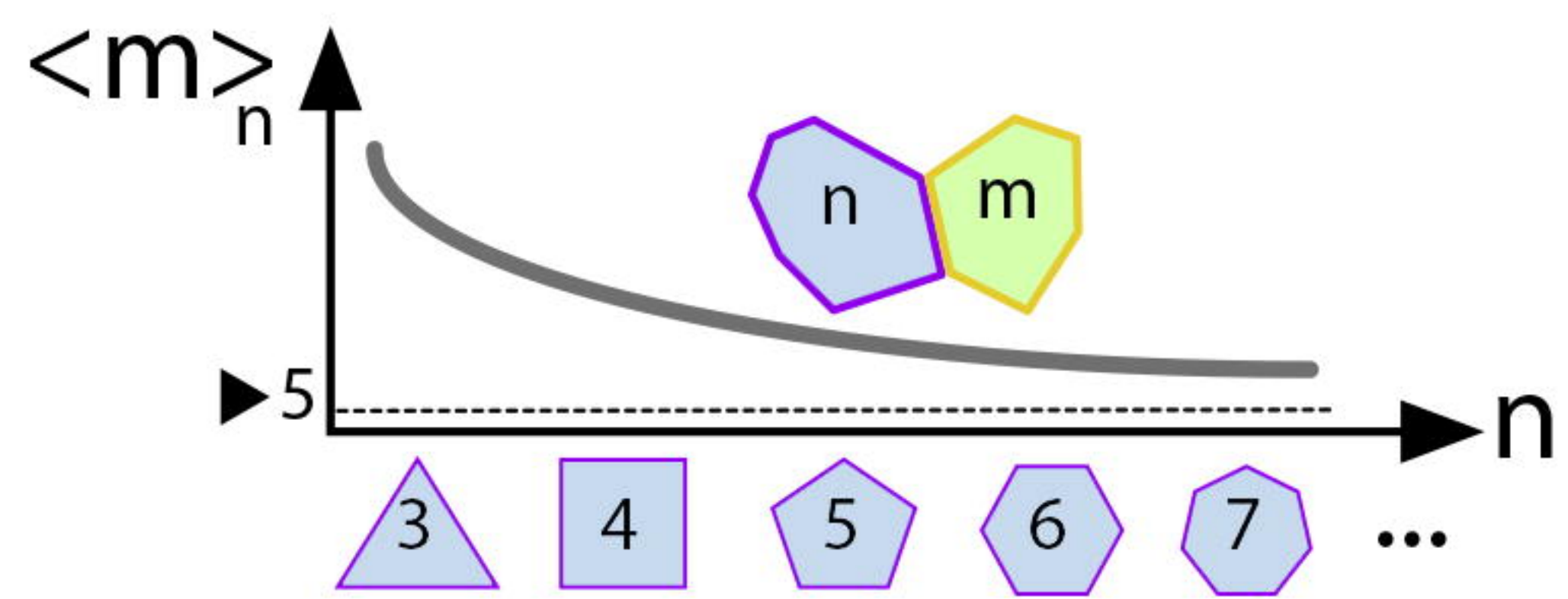
Euler's principle

**C**

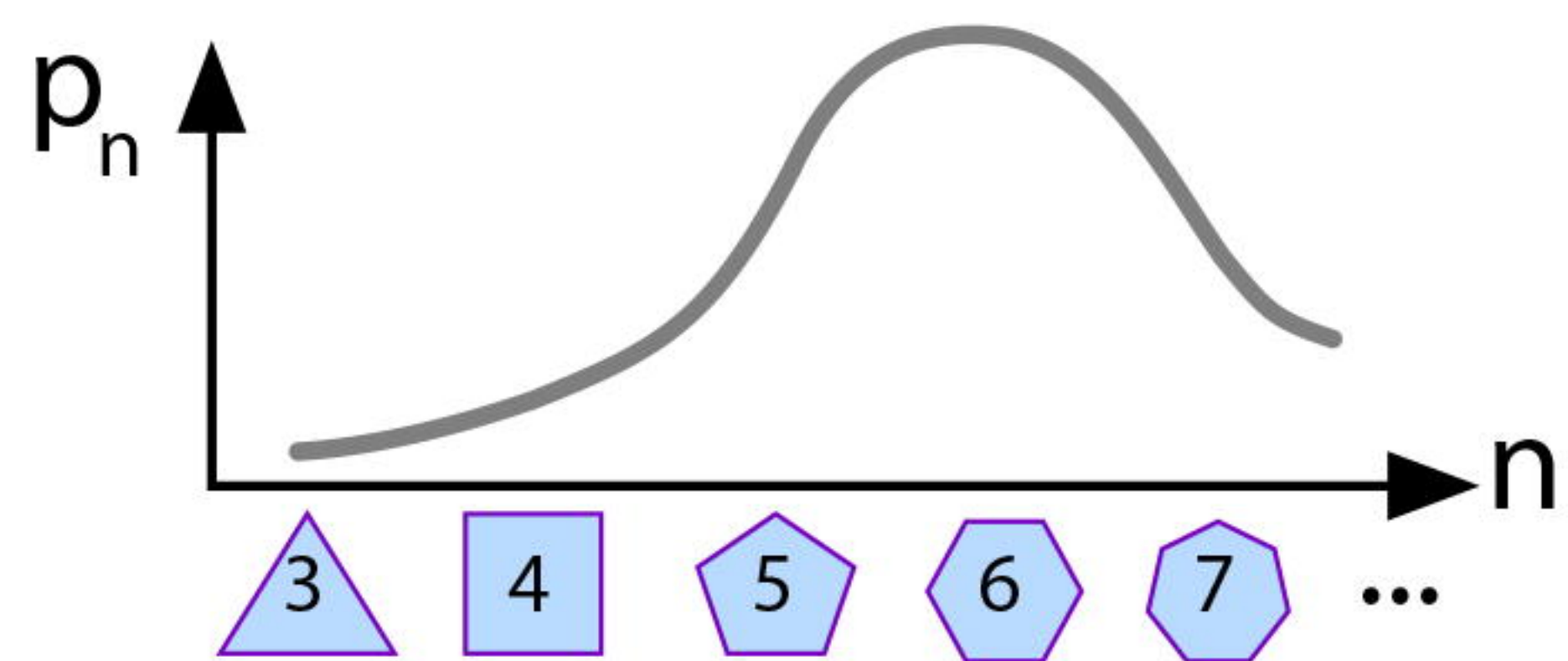
Lewis' law

**D**

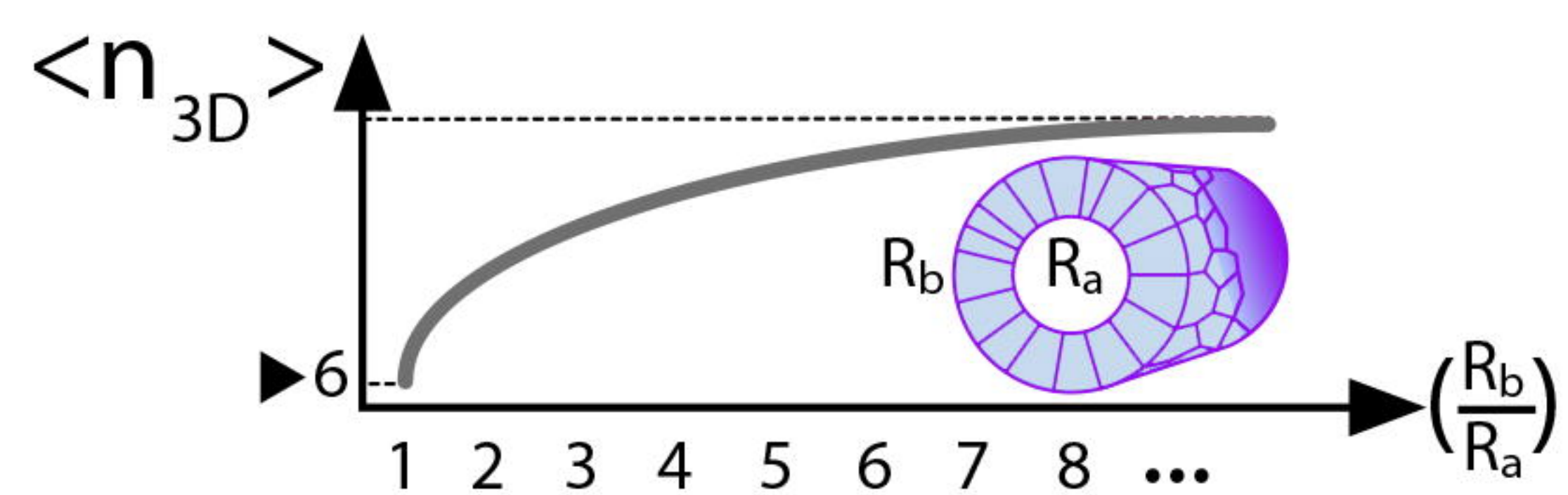
Aboav-Weaire's law

**E**

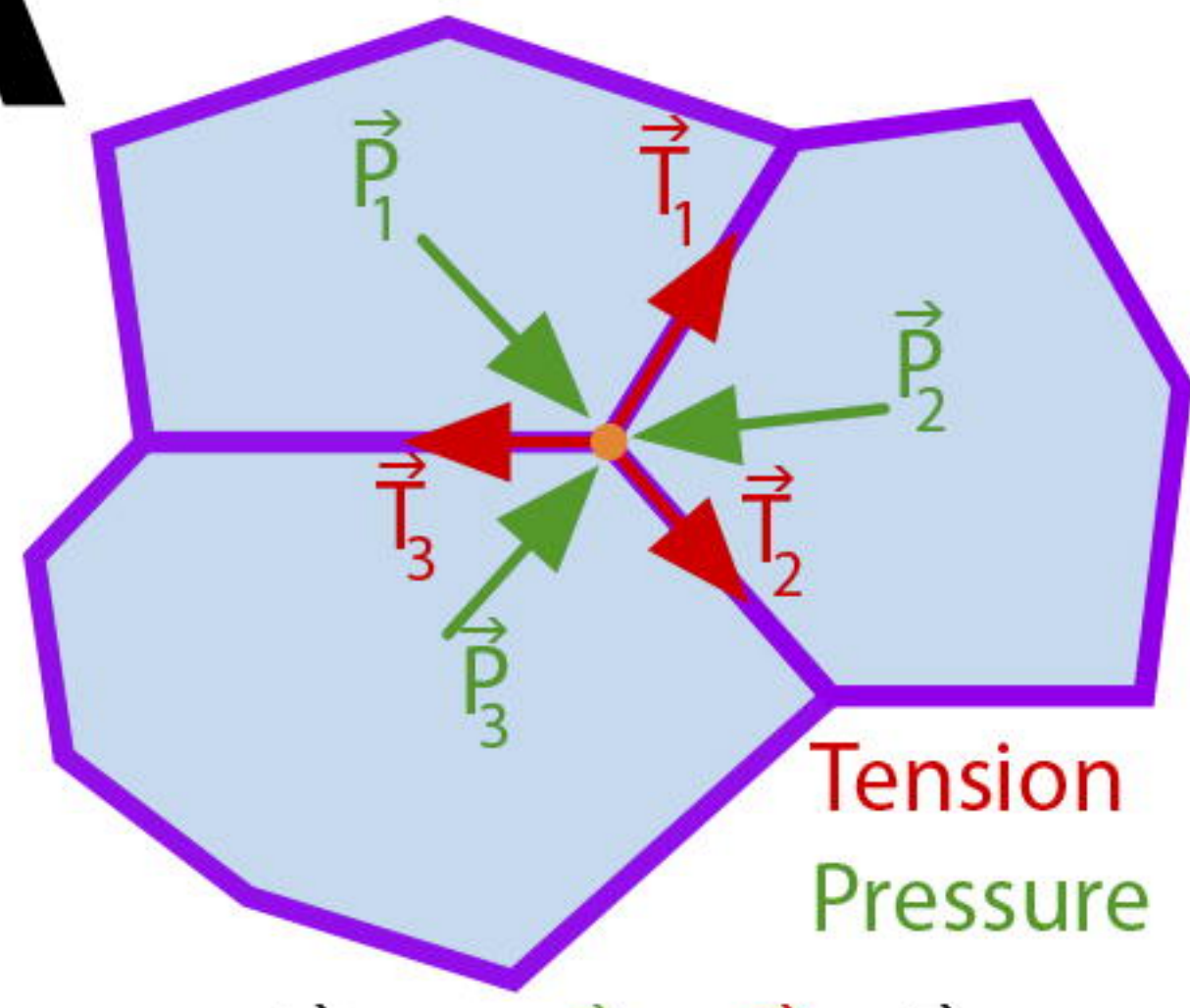
Gibson-Patel's distribution

**F**

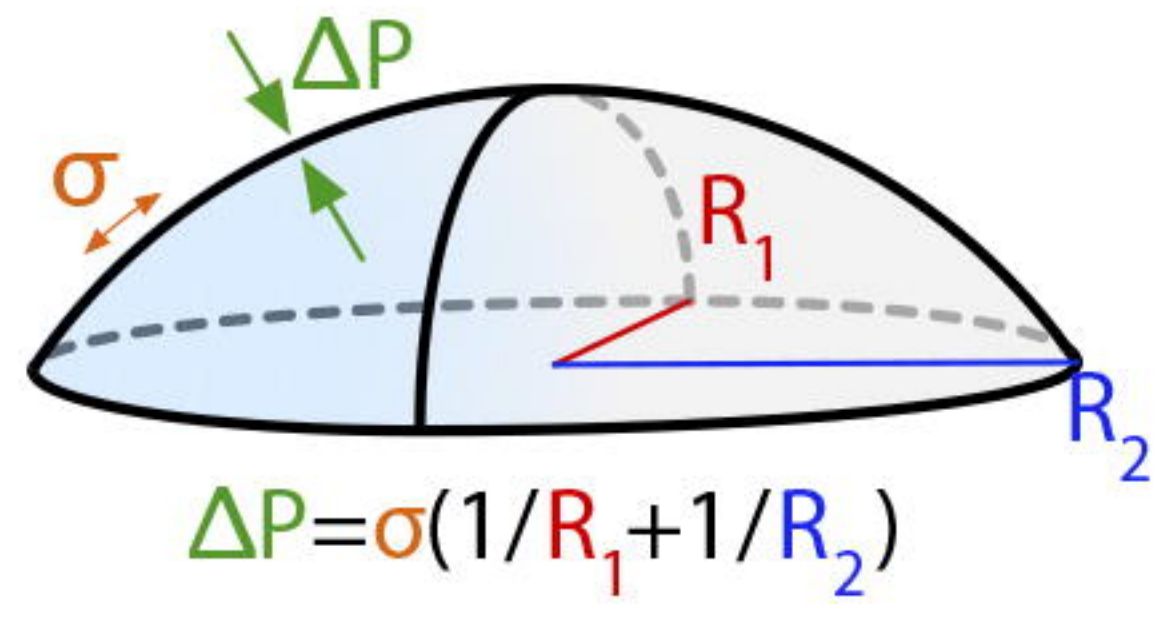
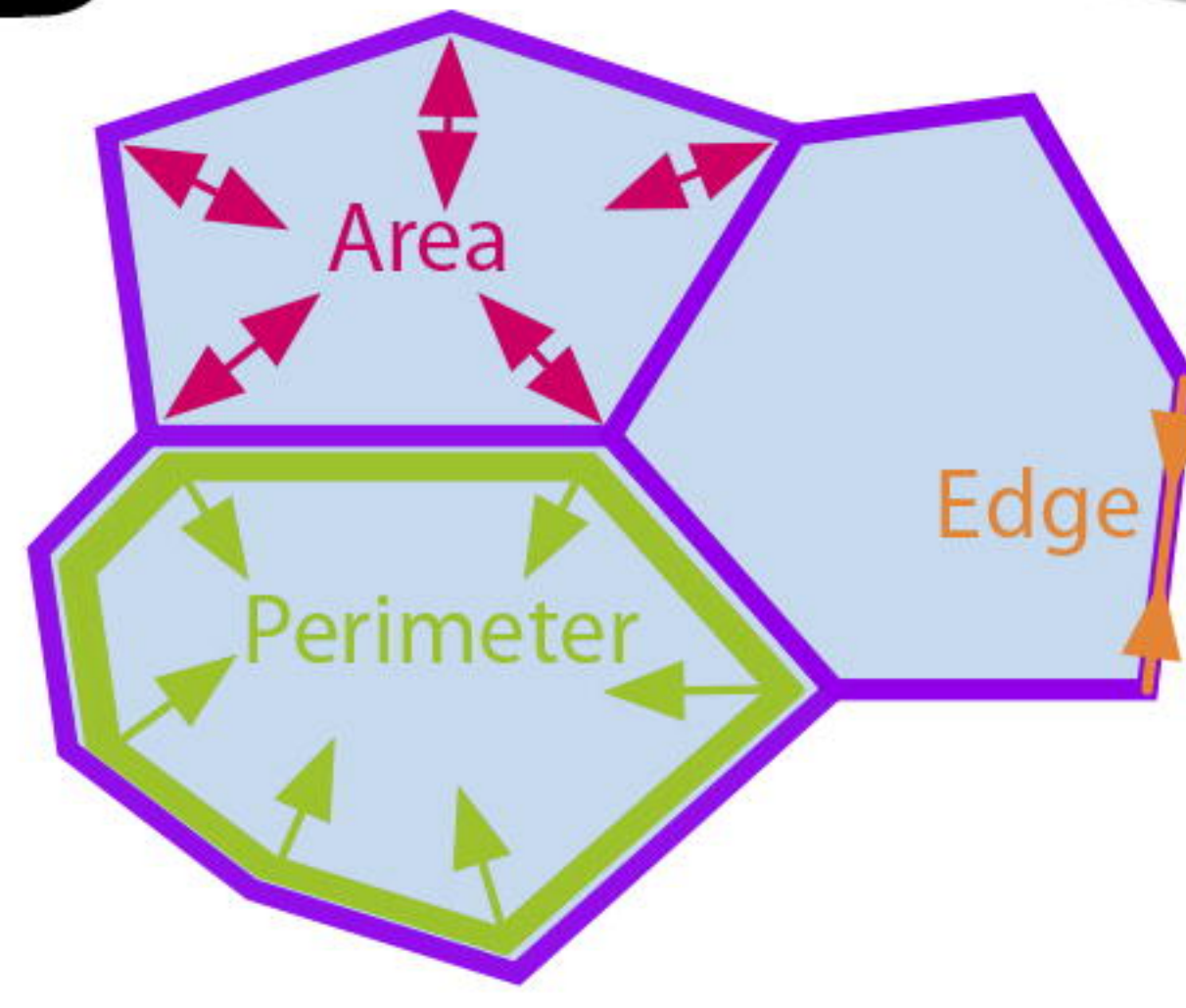
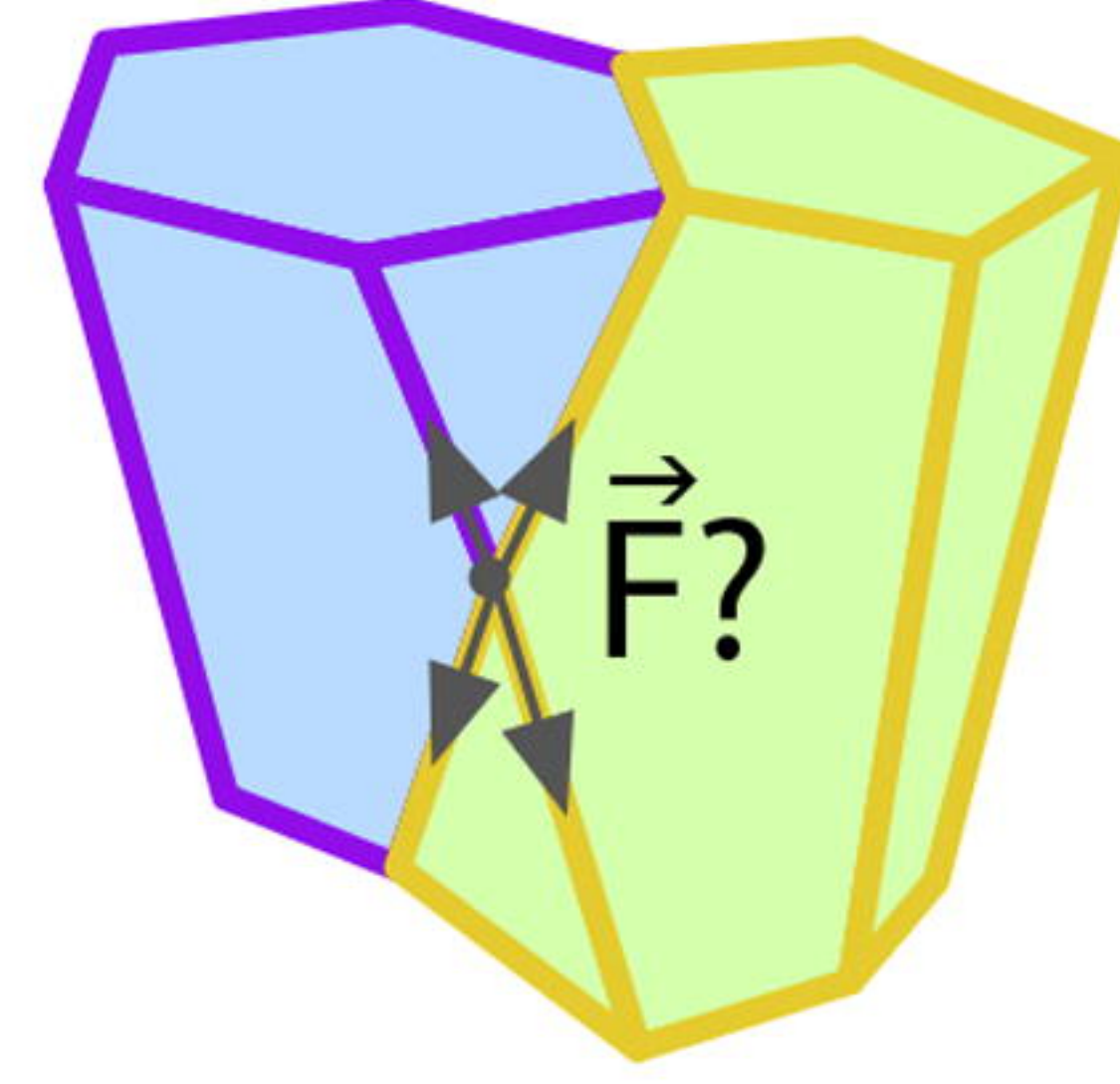
Flintstones' law





**A**

$$\Sigma \vec{F} = \Sigma (A \vec{P} + B \vec{T}) = \vec{0}$$

**B****2D****3D**

- a) Elastic energy:  $\frac{K}{2}(A-A_0)^2$
- b) Contractile energy:  $\frac{\Gamma}{2}L^2$
- c) Adhesion energy:  $\Lambda l$